Accepted Manuscript

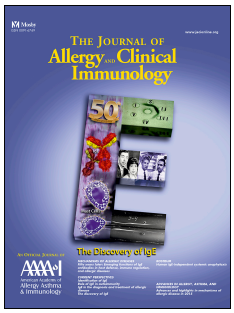

Ectopic Lymphoid Tissues Support Local Immunoglobulin Production in Chronic Rhinosinusitis with Nasal Polyps

Jia Song, M.D., Hai Wang, M.D., Ya-Na Zhang, M.D., Ph.D, Ping-Ping Cao, M.D., Ph.D., Bo Liao, M.D., Ph.D., Zhe-Zheng Wang, M.D., Li-Li Shi, M.D., Ph.D., Yin Yao, M.D., Guan-Ting Zhai, M.D., Zhi-Chao Wang, M.D., Li-Meng Liu, Ming Zeng, M.D., Ph.D., Xiang Lu, M.D., Ph.D., Heng Wang, M.D., Ph.D., Xiang-Ping Yang, Ph.D., Di Yu, Ph.D., Claus Bachert, M.D., Ph.D., Zheng Liu, M.D., Ph.D.

PII: S0091-6749(17)31671-8

DOI: 10.1016/j.jaci.2017.10.014

Reference: YMAI 13092

To appear in: *Journal of Allergy and Clinical Immunology*

Received Date: 18 January 2017

Revised Date: 25 September 2017

Accepted Date: 2 October 2017

Please cite this article as: Song J, Wang H, Zhang Y-N, Cao P-P, Liao B, Wang Z-Z, Shi L-L, Yao Y, Zhai G-T, Wang Z-C, Liu L-M, Zeng M, Lu X, Wang H, Yang X-P, Yu D, Bachert C, Liu Z, Ectopic Lymphoid Tissues Support Local Immunoglobulin Production in Chronic Rhinosinusitis with Nasal Polyps, *Journal of Allergy and Clinical Immunology* (2017), doi: 10.1016/j.jaci.2017.10.014.

Ectopic Lymphoid Tissues Support Local Immunoglobulin Production in Chronic Rhinosinusitis with Nasal Polyps

Jia Song, M.D.[1*], Hai Wang, M.D.[1*], Ya-Na Zhang, M.D., Ph.D [2], Ping-Ping Cao, M.D., Ph.D.[1], Bo Liao, M.D., Ph.D.[1], Zhe-Zheng Wang, M.D.[1], Li-Li Shi, M.D., Ph.D.[1], Yin Yao, M.D.[1], Guan-Ting Zhai, M.D.[1], Zhi-Chao Wang, M.D.[1], Li-Meng Liu[3], Ming Zeng, M.D., Ph.D.[1], Xiang Lu, M.D., Ph.D.[1], Heng Wang, M.D., Ph.D.[1], Xiang-Ping Yang, Ph.D.[4], Di Yu, Ph.D.[5], Claus Bachert, M.D., Ph.D.[6], Zheng Liu, M.D., Ph.D.[1]

[1]Department of Otolaryngology-Head and Neck Surgery, Tongji Hospital, Tongji Medical College, Huazhong University of Science and Technology, Wuhan, P.R. China

[2]Department of Otolaryngology-Head and Neck Surgery, Guangzhou Women and Children's Medical Center, Guangzhou, P.R. China

[3]Li-Meng Liu is a summer student from No.1 Middle School affiliated to Central China Normal University, Wuhan, P.R. China

[4]Department of Immunology, School of Basic Medicine, Tongji Medical College, Huazhong University of Science and Technology, Wuhan, P.R. China

[5]Department of Immunology and Infectious Disease, John Curtin School of Medical Research, Australian National University, Canberra, Australia

[6]Upper Airways Research Laboratory, Ghent University, Ghent, Belgium

* These authors contributed equally to the completion of this article.

Running Head: eLTs in CRSwNP

Word count: 4,157

Disclosure of conflict of interest: None

For correspondence, please contact:

Zheng Liu, MD., Ph.D.

Department of Otolaryngology-Head and Neck Surgery

Tongji Hospital, Tongji Medical College

Huazhong University of Science and Technology

No. 1095 Jiefang Avenue

Wuhan 430030, P.R.China

E-mail: zhengliuent@hotmail.com

Funding: This study was supported by National Natural Science Foundation of China (NSFC) grants 81630024, 81570899 and 81325006 (Z.L.), 81500777 (L.-L.S.), 81400449 (P.-P.C.), and 81670911 (X.L.); the 12th Five Year Science and Technology Support Program (2014BAI07B04); and Australian National Health and Medical Research Council Fellowship to D.Y.

ABSTRACT

Background: The contribution of ectopic lymphoid tissues (eLTs) to local immunoglobulin (Ig) hyperproduction in chronic rhinosinusitis with nasal polyps (CRSwNP) is unclear.

Objective: We sought to explore the cellular basis, formation mechanisms, and function of eLTs in CRSwNP.

Methods: We graded lymphoid aggregations in sinonasal mucosa and histologically studied their structures. The expression of lymphorganogenic factors and molecules required for Ig production was measured using real-time PCR and their localization was analyzed by immunohistochemistry and immunofluorescence. The phenotype of T follicular helper (TFH) cells was analyzed by performing flow cytometry. Ig levels were quantified by using Bio-Plex assay or ImmunoCAP system. Nasal tissue explants were challenged *ex vivo* with *Dermatophagoides pteronyssinus* group 1 (Der p1), and the expression of Iε-Cμ and Iε-Cγ circle transcripts was detected using semi-nested PCR.

Results: Increased formation of eLTs with germinal center-like structures was discovered in eosinophilic (20.69%) and non-eosinophilic CRSwNP (17.31%) compared to chronic rhinosinusitis without nasal polyps (5.66%) and controls (3.70%). The presence of eLTs was associated with increased expression of lymphorganogenic and inflammatory chemokines and cytokines, as well as their receptors. The expression of molecules required for Ig production, the generation of TFH cells, and the production of IgE in eosinophilic polyps and IgG and IgA in both eosinophilic and

non-eosinophilic polyps were predominantly up-regulated in cases with eLTs. After the challenge of Der p1 *ex vivo*, Iε-Cμ transcript was only detected in eosinophilic polyps with eLTs but not in those without eLTs and non-eosinophilic polyps.

Conclusion: eLTs may support local Ig production and therefore significantly contribute to the development of CRSwNP.

Key words: Ectopic lymphoid tissue, immunoglobulin, lymphoid aggregate, lymphorganogenesis.

Clinical implication: Therapeutic strategies that target ectopic lymphoid tissues i**n** nasal polyps may inhibit local immunoglobulin production and disease progression.

Capsule summary: Lymphorganogenic chemokines, survival factors, and lymphotoxin orchestrate the cellular organization of eLTs in nasal polyps, which likely support local Ig production and exacerbate CRSwNP.

Abbreviations:

AID: activation-induced cytidine deaminase

BAFF: B cell-activating factor of the tumor necrosis factor family

Bcl-2: B cell lymphoma 2

CCL19: chemokine (C-C motif) ligand 19

CCL20: chemokine (C-C motif) ligand 20

CCL21: chemokine (C-C motif) ligand 21

CCR6: C-C chemokine receptor 6

CCR7: C-C chemokine receptor 7

CRSwNP: chronic rhinosinusitis with nasal polyps

CRSsNP: chronic rhinosinusitis without nasal polyps

CXCL12: chemokine (C-X-C motif) ligand 12

CXCL13: chemokine (C-X-C motif) ligand 13

CXCR4: C-X-C chemokine receptor 4

CXCR5: C-X-C chemokine receptor 5

DC: dendritic cell

Der p1: *Dermatophagoides pteronyssinus* group 1

ENP: eosinophilic nasal polyp

eLTs: ectopic lymphoid tissues

FDC: follicular dendritic cell

GC: germinal center

HEV: high endothelial venule

Ig: immunoglobulin

ICAM1: intercellular adhesion molecule 1

ICOS: inducible costimulator

LIGHT: tumor necrosis factor superfamily member 14

LTα: lymphotoxin alpha

LTβ: lymphotoxin beta

LTβR: lymphotoxin beta receptor

NENP: non-eosinophilic nasal polyp

NP: nasal polyp

PD1: programmed cell death protein

PNAd: peripheral node addressin

TFH: T follicular helper

VCAM1: vascular cell adhesion molecule 1

INTRODUCTION

Chronic rhinosinusitis with nasal polyps (CRSwNP) is characterized by exaggerated inflammation in sinonasal mucosa and formation of polyps.[1] Medical treatments usually involve nonspecific suppression of chronic inflammation and are ineffective in many patients, reflecting our limited understanding of the complicated cellular and molecular networks in CRSwNP.[1] An array of evidence has implicated a critical role of local immunoglobulin (Ig) hyperproduction in the pathogenesis of CRSwNP.[2, 3] IgE antibodies against aeroallergens and *Staphylococcus aureus* enterotoxins were identified in nasal polyps (NPs), which could activate mast cells upon allergen exposure and were correlated with local eosinophilia.[4, 5] Additionally, autoreactive antibodies, such as anti-double stranded DNA IgG and anti-BP180 IgG, have recently been demonstrated in NPs and potentially linked with mucosal complement activation.[6-8] Increased IgA levels have also been reported in NPs and may contribute to eosinophil activation.[9] Importantly, higher local IgE and IgG levels were found to associate with poorly controlled disease in CRSwNP patients even after surgical intervention.[4, 6]

Currently, the mechanisms underlying local Ig hyperproduction in CRSwNP are poorly understood. Antigen-driven antibody affinity maturation, isotype switch, and memory formation usually take place within germinal centers (GC) formed in secondary lymphoid organs such as spleens or lymph nodes. Nevertheless, increased accumulation and activation of B cells, driven by up-regulated expression of B-cell chemokines and activating factors, have been demonstrated in NPs.[9, 10] Local IgE levels were up-regulated in patients with eosinophilic CRSwNP independent of

systemic atopy.[4, 11] Moreover, receptor revision and class switching to IgE could occur in NPs, implicating a potential local antibody response and GC reaction in NPs.[11, 12] Indeed, ectopic lymphoid tissues (eLTs) have been found in NPs.[13-16] However, the cellular basis, formation mechanisms, and function of polyp eLTs remain to be defined.

The purpose of this study was to investigate (1) the size and structure of lymphoid aggregates in NPs and their frequency in patients, and the relationship between lymphoid aggregates and eLTs characterized by the presence of GC-like structures; (2) the potential mechanisms underlying the lymphoid neogenesis in NPs, and (3) the function of eLTs in local Ig production and its clinical relevance in CRSwNP.

METHODS

Subjects

This study was approved by the Ethics Committee of Tongji Hospital and conducted with written informed consent from each patient. The diagnosis of CRSwNP and chronic rhinosinusitis without nasal polyps (CRSsNP) was made according to the current European Position Paper on Rhinosinusitis and Nasal Polyps (EPOS).[1] CRSwNP was defined as eosinophilic when the percentage of tissue eosinophils exceeded 10% of total infiltrating cells, as reported by our previous study.[17] This cut-off was calculated as twice the standard deviation of the mean of eosinophil percentages in controls.[17] Subjects undergoing septoplasty because of

anatomic variation and without other sinonasal diseases were enrolled as controls.[11, 17] Polyp tissues from CRSwNP patients, diseased sinus mucosa from CRSsNP patients, and inferior turbinate mucosal tissues from control subjects were obtained during surgery. Demographic characteristics of enrolled subjects are listed in Table E1, and additional information is provided in this article's Online Repository.

Histology study

Tissue sections were stained with hematoxylin-eosin, and lymphocyte aggregation was graded according to a previously described method.[18, 19] Each sample was graded according to the highest level of lymphoid aggregation present.[18] Cell aggregates with a radial cell count between 2 and 5 cells were classified as Grade 1, those with 6 to 10 cells were classified as Grade 2, while those with more than 10 radial cells were classified as Grade 3.[18, 19] The number of lymphoid aggregates was counted at a low power magnification (× 100). More information is provided in this article's Online Repository.

Immunohistochemistry and immunofluorescence

Structures of lymphoid aggregates were evaluated by immunohistochemistry and immunofluorescence as previously described in prior researches.[17, 20-22] Antibodies used are listed in Tables E2 and E3. More information is provided in this article's Online Repository.

Measurement of Igs, chemokines and cytokines

Ig and chemokine levels in tissues, and cytokine levels in culture supernatants were detected by using ImmunoCAP system, Bio-Plex assay, Q-Plex assay, or ELISA as previously reported.[11, 15, 23, 24] More information is provided in this article's Online Repository including Tables E4-E6.

Reverse transcription polymerase chain reaction

Quantitative RT-PCR was performed with specific primers (Table E7) as stated elsewhere.[11, 17] The specific circle transcripts Iε-Cμ, Iε-Cγ, Iε-Cγ1, Iε-Cγ3, and Iε-Cγ4 were investigated using a semi-nested PCR with appropriate primers (Table E8) as previously described.[11, 25] More information is provided in this article's Online Repository.

***Ex vivo* allergen challenge**

Sinonasal mucosal tissues obtained from 5 controls without local specific IgE (sIgE) against *Dermatophagoides pteronyssinus* group 1 (Der p1) and not having eLTs, 9 eosinophilic CRSwNP patients with local sIgE against Der p1 (5 of them having eLTs in NPs), and 8 non-eosinophilic CRSwNP patients without local sIgE against Der p1 (4 of them having eLTs in NPs) were subject to *ex vivo* air-liquid interface culture.[25-27] Tissue explants were stimulated with recombinant Der p1 (20 μg/mL, endotoxin ≤ 0.03 EU/μg; Indoor Biotechnologies, Charlottesville, VA, USA) for 24 hours as mentioned previously.[25-27] After stimulation, tissue explants and culture

supernatants were harvested for further analysis. More information is provided in this article's Online Repository.

Flow cytometry

The flow cytometric analysis of nasal mucosal mononuclear cells (NMCs) was performed as previously described.[15, 20] More information is provided in this article's Online Repository including Table E9.

Statistics

Statistical analysis was performed using the SPSS 18.0 software (SPSS Inc., Chicago, IL, USA). For continuous variables, results are presented in dot plots unless specifically stated. Symbols represent individual samples; horizontal bars represent medians, and error bars show interquartile ranges. When comparisons were made between groups, the Kruskal-Wallis *H* test was used to assess significant intergroup variability. The Mann-Whitney *U* 2-tailed test was used for between-group comparison. Chi-square test or Fisher's exact test was applied to compare the differences in proportions between groups. Spearman rank test was used for correlations. Significance was accepted at $P < 0.05$.

RESULTS

Increased formation of lymphoid aggregates in NPs

We analyzed a large cohort of surgical samples from patients with eosinophilic

and non-eosinophilic CRSwNP using hematoxylin-eosin staining and found that lymphoid aggregates were present in about half of the samples, in contrast to 19.26% of control samples (Fig E1, A-C). Lymphoid aggregates were graded on size. Lymphoid aggregates of each grade were found in higher frequency in eosinophilic and non-eosinophilic NPs as compared with controls (Fig E1, C and Table E10). Consistently, eosinophilic or non-eosinophilic NPs samples had higher numbers of lymphoid aggregates, as compared with controls, by total numbers or numbers of each grade (Fig E1, D). In some samples, aggregates in different grades could be discovered simultaneously (Fig E1, E).

Diversified structures of lymphoid aggregates in NPs

We investigated the structures of lymphoid aggregates in different grades by immunostaining samples from a subgroup of subjects, using tonsils as staining positive controls (Fig E2). We found that lymphoid aggregates in the same grade usually displayed a similar structure. There was no noticeable difference in the structures between lymphoid aggregates in eosinophilic and non-eosinophilic NPs (Table 1). Lymphoid aggregates with GC-like structures, characterized by the presence of Ki-67$^+$ proliferating B cells, CD21$^+$ follicular dendritic cell (FDC) networks, and peripheral node addressin (PNAd)$^+$ high endothelial venules (HEVs), were defined as eLTs (Fig 1).[19] We found that eLT development was associated with larger lymphoid aggregation, i.e. higher grade (Table 1). The eLTs were discovered in the majority of grade 2 (64.29%) and 3 (92.31%) lymphoid aggregates but absent in

grade 1 lymphoid aggregates (Table 1). The eLTs presented more frequently in eosinophilic (20.69%) and non-eosinophilic NPs (17.31%) compared with controls (3.70%) (Fig 2). No increase of eLT formation was found in diseased sinus mucosa from CRSsNP patients (5.66%) (Fig 2). In addition to HEVs, lymphatic vessels were also found in eLTs (Fig 1, B). HEVs were typically observed inside follicles, whereas lymphatic vessels were found mostly surrounding the follicles, in polyp eLTs (Fig 1, B). These specialized vascular and canalicular systems are essential for regulating leukocyte traffic and compartmentalization. In polyp eLTs, $CD11c^+$ DCs infiltrated in follicles, and $CD138^+$ plasma cells were found surrounding the follicles (Fig 1, B and D). In addition, innate immune cells including $CD68^+$ macrophages and $CD56^+$ natural killer cells were found inside or surrounding the follicles (Fig 1, B). Compared with follicles in tonsils, polyp eLTs did not have clear T-cell zone and polarized B-cell follicle (Fig 1 and Fig E2).

Up-regulated expression of lymphorganogenic chemokines and cytokines in eLTs in NPs

The formation of eLTs is initiated by the local recruitment and compartmentalization of T cells, B cells, and DCs under the coordination of homeostatic chemokines.[28, 29] In order to investigate the potential mechanisms underlying the lymphoid neogenesis in NPs, we investigated the association between eLT formation and mRNA expression of chemokine (C-X-C motif) ligand 12 (CXCL12)/C-X-C chemokine receptor 4 (CXCR4), CXCL13/CXCR5, chemokine

(C-C motif) ligand 20 (CCL20)/C-C chemokine receptor 6 (CCR6), and CCL19 and CCL21/CCR7 in NPs. Compared with those without eLTs or control samples, the mRNA expression levels of all tested chemokines and chemokine receptors were comparably elevated in eosinophilic and non-eosinophilic NPs with eLTs except for CXCL12 and CCL20 (Fig 3, A). We further measured the tissue protein levels of CXCL13 and CCL21, two critical chemokines for lymphoid organ formation, and confirmed their increased expression in NPs with eLTs (Fig E3). Immunohistochemistry and immunofluorescence demonstrated that CXCL13 was mainly expressed by FDCs and B cells inside follicles and CCL21 expression was mostly observed in endothelial cells surrounding the follicles in areas where HEVs and lymphatic vessels were observed in polyp eLTs (Fig 3, B and C). $CXCR5^+$ B cells and $CCR7^+$ T cells were enriched within polyp eLTs (Fig 3, D). In addition to eLTs, scattered $CXCL13^+$ mononuclear cells, $CCL21^+$ stromal cells, $CXCR5^+$ cells, and $CCR7^+$ cells were also discovered in other areas in polyps (Fig E4).

The expression of lymphorganogenic chemokines is usually under the control of lymphotoxin (LT) β receptor (LTβR) signaling.[28-30] LTβR signaling is also crucial for the expression of enzymes regulating PNAd expression.[31] We found that eosinophilic and non-eosinophilic NPs with eLTs had comparably up-regulated mRNA expression of LTβR ligands including LTα, LTβ and tumor necrosis factor superfamily member 14 (LIGHT) compared with NPs without eLTs and controls (Fig 4, A). Consistently, the protein levels of LTα were up-regulated in eosinophilic and non-eosinophilic NPs with eLTs (Fig E3). In addition, we discovered the presence of LTα, LTβ, and LTβR

expressing cells inside and surrounding the follicles in polyp eLTs (Fig 4, B). LTβR$^+$ B cells were mainly detected in follicles and a few of them were also found in other areas besides eLTs in polyps (Fig 4, C and Fig E4). Recent studies suggest that IL-17 may contribute to the development of eLTs in chronically inflamed tissues.[32] Th17 cells and IL-17 are able to trigger maturation of FDC network and upregulate the expression of CXCL13 and CCL19 independent of lymphotoxin.[29, 33] Our previous studies reported the accumulation of Th17 cells in NPs.[20, 34] In the present study, we further found that the mRNA expression of IL-17A, IL-17F and their receptor (IL-17RA) was mainly up-regulated in eosinophilic and non-eosinophilic NPs with eLTs, and no significant difference was found between two types of NPs (Fig 4, A). IL-17A$^+$ cells were identified inside and surrounding the eLTs and in other areas in polyps (Fig 4, C and Fig E5). Compared with controls, the number of IL-17A$^+$ cells was increased in both eosinophilic and non-eosinophilic polyps with a more prominent increase in those with eLTs (Fig E5). As another cytokine involved in the initiation and maintenance of eLTs within tissues,[29] IL-7 is considered to promote lymphocyte survival by inducing the expression of anti-apoptotic factor B cell lymphoma 2 (Bcl-2) and to regulate early lymphatic vessel expansion.[21] We found that both IL-7 and IL-7R mRNA levels were up-regulated similarly in eosinophilic and non-eosinophilic NPs with eLTs compared with controls and NPs without eLTs (Fig 4, A). Immunofluorescence demonstrated IL-7 expression in eLTs and scattered IL-7$^+$ cells were also found in other locations other than eLTs (Fig 4, C and Fig E6). HEVs express adhesion molecules, such as intercellular adhesion molecule 1 (ICAM1)

and vascular cell adhesion molecule 1 (VCAM1), which promote the accumulation of naïve lymphocytes from the blood.[28, 29] We found that the mRNA expression of ICAM1 and VCAM1 was enhanced in NPs with eLTs compared with controls or NPs without eLTs (Fig 4, A). Although ICAM1 and VCAM1 positive vessels were distributed throughout lamina propria of nasal tissues (Fig E7), their expression was enriched in polyp eLTs in areas where HEVs were observed (Fig 4, D).

Polyp eLTs correlated to local production of IgG, IgE, and IgA but not IgM

Given the hyperproduction of several Ig isotypes in NPs, we next tested the notion that eLTs can support local Ig production. T follicular helper (TFH) cells in GCs regulate B cell somatic hypermutation and provide B cells with necessary signals for Ig isotype switching and memory formation.[35] TFH cells up-regulate the expression of CXCR5, inducible costimulator (ICOS), programmed cell death protein (PD1), transcription factor Bcl-6, and IL-21 to enable their function.[35] Consistent with our previous report,[15] $CXCR5^+CD4^+$ TFH cells were identified in B-cell areas in polyp eLTs (Fig 5，A). Using flow cytometry, we further found a similar increase of frequencies of total TFH cells, $ICOS^+$ TFH cells, $PD\text{-}1^+$ TFH cells, $ICOS^+PD\text{-}1^+$ TFH cells, and $IL\text{-}21^+$ TFH cells in NMCs from eosinophilic and non-eosinophilic NPs with eLTs in comparison with those from NPs without eLTs and controls (Fig 5, B). Notably, the expression of ICOSL and IL-21 was up-regulated in TFH cells from NPs with eLTs compared with those from NPs without eLTs and control mucosa, suggesting an increased activity of TFH cells in polyp eLTs (Fig E8).

Moreover, we found that NPs with eLTs had higher mRNA levels of activation-induced cytidine deaminase (AID, an enzyme required for somatic hypermutation and isotype class-switch of GC B cells), CD21L (a marker for FDC), and B-cell activating factor of the tumor necrosis factor family (BAFF, a B-cell survival promoting factor) than NPs without eLTs and controls (Fig 5, C). There were positive correlations between CD21L and BAFF, CD21L and AID, and BAFF and AID expression in polyps with eLTs (Fig E9), suggesting a potential role of BAFF and FDC on AID expression and Ig class switch in B cells. By immunohistochemical staining, we confirmed the predominant expression of AID and BAFF in follicles of polyp eLTs (Fig 5, D). CD23 is required for the survival and differentiation of GC B cells. $CD23^+$ B cells and FDCs in polyp eLTs were demonstrated by immunofluorescence (Fig 5, E). Consistent with up-regulated IL-7 and BAFF signals in polyp eLTs, we observed $Bcl\text{-}2^+$ cells in the periphery of follicles of polyp eLTs (Fig 5, D).

After defining the presence of cellular and molecular components required for Ig class switching in polyp eLTs, we explored the potential function of eLTs in local Ig production in polyps. Consistent with our previous report,[15] we found that IgE levels were increased in eosinophilic NPs, and IgA and IgG levels were up-regulated in both eosinophilic and non-eosinophilic NPs, in comparison with controls, while IgM levels were comparable (Fig E10). Importantly, we found that IgE levels were prominently increased in eosinophilic NPs, and total IgG and IgA levels were up-regulated in both eosinophilic and non-eosinophilic NPs with eLTs compared with those without eLTs,

respectively (Fig 6, A). Compared with controls, no increase of IgM levels was found in polyps with or without eLTs (Fig 6, A), suggesting that eLTs are more essential for the production of isotype class-switched antibodies. Immunofluorescence showed that IgM was mainly expressed by $CD20^+$ B cells but not plasma cells in eLTs, suggesting that IgM^+ cells are potentially IgM^+ unswitched B cells (Fig 6, B). In contrast, IgE^+, IgA^+, and IgG^+ plasma cells were readily detected, and a few IgE^+, IgA^+, and IgG^+ B cells were found in polyp eLTs (Fig 6, B). In addition, IgE staining was also co-localized with some DCs, FDCs, and $tryptase^+$ mast cells (Fig 6, C).

In order to gain direct evidence that polyp eLTs support local Ig production, we performed an *ex vivo* challenge assay. After the *ex vivo* stimulation with Der p1, the specific circle transcript of Iε-Cμ (408 bp) produced during class-switch recombination from IgM to IgE was detected in 4 of 5 eosinophilic NPs with local sIgE against Der p1 and eLTs (Fig 6, D). Iε-Cμ circle transcript was also detected in 1 non-stimulated eosinophilic NP with eLTs. However, no Iε-Cμ circle transcript was detected in 4 eosinophilic NPs having local sIgE against Der p1 but without eLTs before or after stimulation. For 8 non-eosinophilic NPs without local sIgE against Der p1, no Iε-Cμ circle transcript was detected regardless of the presence of eLTs. No Iε-Cμ circle transcript was detected in 5 controls either (Table E11). No Iε-Cγ circle transcript (339 bp) produced from any subclass of IgG to IgE, or Iε-Cγ1, Iε-Cγ3 or Iε-Cγ4 circle transcript (339 bp) produced from specific IgG subclass to IgE was detected in any samples (Table E11). After stimulation, protein levels of IL-4, IL-5, IL-13, and IL-17A in the supernatant were significantly increased in eosinophilic NPs

with eLTs, but not in eosinophilic NP without eLTs or controls (Fig E11). In contrast, for non-eosinophilic NPs, no significant change of those cytokines was found after stimulation regardless of the presence of eLTs (Fig E12).

The formation of eLTs associated with disease severity

Finally, we examined the association between eLT formation and objective CRS severity, symptom severity, disease duration, prior surgery, asthma, and allergic rhinitis, and we found longer disease duration, more severe nasal obstruction, and higher frequency of prior surgery in patients with eLTs compared with those without eLTs (Table E12).

DISCUSSION

Although the infiltration of immune cells and the formation of lymphoid aggregates have been reported in NPs, the characteristics of lymphoid aggregates, immunological mechanism for the formation, and their functions have not been well determined. This is the first study that demonstrates the presence of lymphoid aggregates with different sizes and features in over half of both eosinophilic and non-eosinophilic NPs. The simultaneous presence of lymphoid aggregates in various grades reflects a dynamic process of lymphoid neogenesis in NPs (Fig E1). Larger lymphoid aggregates demonstrated relatively well-developed structures (Table 1). The majority of grade 2 and grade 3 aggregates developed into eLTs. The eLTs were found in about 20% of CRSwNP patients but were almost absent in controls and CRSsNP

patients (Fig 2). A very recent study demonstrated the presence of eLTs in 37% of polyps but in none of normal ethmoid mucosa, slightly higher than our results.[16] This might be due to less stringent criteria using hematoxylin-eosin staining,[16] as compared to a more comprehensive validation by immunohistochemistry in our study. A similar finding of increased formation of lymphoid structures in polyps was also reported by Shinoda et al.[36] In contrast, Feldman et al. did not show a difference in B cell follicles or B cell clusters in polyps compared to normal ethmoid tissues.[37] The reasons for those discrepancies are unclear currently; however, Feldman et al. did not investigate the structures of follicles in detail, including the presence of HEVs and FDCs.[37] Here, we did not find a difference in the frequency of eLT formation between eosinophilic and non-eosinophilic NPs, suggesting that multiple up-stream factors can initiate eLT formation in chronically inflamed tissues. The formation of lymphoid aggregates in NPs is unlikely due to the co-existence of allergic rhinitis and asthma, since CRSwNP patients without allergic rhinitis and asthma also demonstrated a significantly higher frequency of lymphoid aggregates compared with controls (data not shown).

The expression of eLT related genes in CRSwNP has been investigated previously,[10, 16] but the association between the expression of those genes and formation of eLTs remains undetermined. Our study for the first time revealed a significant association between eLT formation, expression of homeostatic chemokines and chemokine receptors, and up-stream lymphorganogenic signaling pathways in CRSwNP (Figs 3 and 4). Interestingly, although previous studies demonstrated different immunological conditions in eosinophilic and non-eosinophilic NPs,[17] we

found that they shared similar lymphoid neogenesis and compartmentalization pathways in the development of eLTs (Figs 3 and 4). It suggests that different disease initiators may activate similar downstream lymphoid neogenesis pathways in eosinophilic and non-eosinophilic polyps. In fact, IL-17, CXCL13, and LT are similarly implicated in the development of eLTs in different diseases and inflammatory conditions including autoimmune diseases, chronic obstructive pulmonary disease, and pulmonary inflammation induced by bacteria and viruses.[38-41] However, the relative contributions of each individual molecule and their inter-regulation in the formation of polyp eLTs are topics to be studied in the future. It should be noted that expression of those molecules was also found in other areas of polyps besides eLTs (Figs E4-E7), suggesting additional functions beyond eLT formation for those molecules in the pathogenesis of NPs.[20, 34, 36, 42-45] Type 17 response was absent in tissue samples from European and North American patients with polyps in contrast to Chinese patients with polyps.[23, 46, 47] On the other hand, IL-17 was highly detected in CRSsNP where no up-regulation of eLT formation was found.[23, 47] Therefore, the role of IL-17 in the development of eLTs in NPs requires further investigation.

In regards to the previously unknown function of polyp eLTs, our study provides several lines of novel evidence for the regulatory role of eLTs in local Ig production in NPs. First, we identified the presence of cellular and molecular elements essential for B cell differentiation and activation as well as *in situ* antibody diversification and isotype switching in polyp eLTs, including TFH cells, AID, BAFF, and CD23. The

463 expression levels of those cellular and molecular components were related to the
464 presence of eLTs in NPs (Fig 5). Second, we found that local hyperproduction of IgE,
465 IgG, and IgA was more prominent in NPs with eLTs than that in NPs without eLTs
466 (Fig 6, A). In addition, IgA, IgG, and IgE-producing plasma cells could be detected in
467 polyp eLTs, confirming the local Ig production in polyp eLTs (Fig 6, B). Third, most
468 importantly, we demonstrated ongoing Ig class-switch recombination to IgE only in
469 eosinophilic polyps with eLTs, but not in those without eLTs after *ex vivo* stimulation
470 with specific allergens (Fig 6, D and Table E11). The *ex vivo* tissue challenge assay
471 allowed us to confirm the intrinsic origin of Ig production of eLTs. In this study, we
472 failed to observe clear expression of Iε-Cγ circle transcript after stimulation,
473 disfavoring the sequential switching to IgE through IgG in NPs. Stimulation with
474 specific antigen also led to production of IL-4 and IL-13 in eosinophilic NPs with
475 eLTs, which are strong inducers of IgE switch.[25, 27] In polyps without eLTs, we also
476 detected enhanced levels of IgE, IgG, and IgA compared with controls. It is possible
477 that B cells already committed to Ig synthesis in secondary lymphoid organs are
478 recruited to the inflamed NPs and contribute to local Ig production. We cannot rule
479 out the possibility that Igs produced in secondary lymphoid organs circulate to NPs
480 either. Nevertheless, our findings clearly demonstrate an important contribution of
481 eLTs to local Ig in NPs. In this study, we found that IgE was only up-regulated in
482 eosinophilic NPs with eLTs, suggesting that distinct external pathogenic stimulators
483 and intrinsic responses would determine the function of eLTs in subjects with different
484 types of CRSwNP. The pathological role of local IgE in the eosinophilic inflammation

in NPs has been revealed by several previous studies.[5, 11, 14, 15] However, the antigen specificity of IgG and IgA and their roles in the pathogenesis of NPs are poorly understood and deserve more studies in the future.[6-8]

Based on this prospective study with large sample size, we found that eLT formation was associated with a higher frequency of prior surgery, suggesting that eLTs may affect disease progression. One limitation of our study is to use inferior turbinate mucosal samples as controls for NPs. However, the limited amount of ethmoid tissues does not allow us to perform extensive studies. In fact, we did not find significant formation of lymphoid aggregates, especially eLTs, in normal ethmoid mucosal samples with a small sample size (Fig E13). Another limitation is that we did not investigate the production of different IgG subclasses. Clearly, different IgG subclasses may have distinct functions, and this study is currently in progress in our lab.

In conclusion, NPs have up-regulated formation of eLTs under chronic inflammation. Homeostatic chemokines, LTβR signaling, and survival factors are involved in the development of eLTs in both eosinophilic and non-eosinophilic NPs. Polyp eLTs support local Ig production and contribute to disease progression of NPs (Fig 7). Despite the limits inherent to studies in humans, in this study, we provided novel insights into the formation and function of eLTs in NPs and underscored that eLTs might be a potential therapeutic target to control inflammation in CRSwNP. It would be interesting to investigate whether steroids diminish the formation of eLTs in CRSwNP patients.

REFERENCES

1. Fokkens WJ, Lund VJ, Mullol J, Bachert C, Alobid I, Baroody F, et al. European Position Paper on Rhinosinusitis and Nasal Polyps 2012. Rhinol Suppl 2012:3 p preceding table of contents, 1-298.

2. Stevens WW, Lee RJ, Schleimer RP, Cohen NA. Chronic rhinosinusitis pathogenesis. J Allergy Clin Immunol 2015; 136:1442-53.

3. Min JY, Hulse KE, Tan BK. B-cells and antibody-mediated pathogenesis in chronic rhinosinusitis with nasal polyps. Adv Otorhinolaryngol 2016; 79:48-57.

4. Van Zele T, Gevaert P, Watelet JB, Claeys G, Holtappels G, Claeys C, et al. Staphylococcus aureus colonization and IgE antibody formation to enterotoxins is increased in nasal polyposis. J Allergy Clin Immunol 2004; 114:981-3.

5. Zhang N, Holtappels G, Gevaert P, Patou J, Dhaliwal B, Gould H, et al. Mucosal tissue polyclonal IgE is functional in response to allergen and SEB. Allergy 2011; 66:141-8.

6. Tan BK, Li QZ, Suh L, Kato A, Conley DB, Chandra RK, et al. Evidence for intranasal antinuclear autoantibodies in patients with chronic rhinosinusitis with nasal polyps. J Allergy Clin Immunol 2011; 128:1198-206 e1.

7. De Schryver E, Calus L, Bonte H, Natalie de R, Gould H, Donovan E, et al. The quest for autoreactive antibodies in nasal polyps. J Allergy Clin Immunol 2016; 138:893-5 e5.

8. Van Roey GA, Vanison CC, Wu J, Huang JH, Suh LA, Carter RG, et al.

Classical complement pathway activation in the nasal tissue of patients with chronic rhinosinusitis. J Allergy Clin Immunol 2017; 140:89-100 e2.

9. Kato A, Peters A, Suh L, Carter R, Harris KE, Chandra R, et al. Evidence of a role for B cell-activating factor of the TNF family in the pathogenesis of chronic rhinosinusitis with nasal polyps. J Allergy Clin Immunol 2008; 121:1385-92, 92 e1-2.

10. Patadia M, Dixon J, Conley D, Chandra R, Peters A, Suh LA, et al. Evaluation of the presence of B-cell attractant chemokines in chronic rhinosinusitis. Am J Rhinol Allergy 2010; 24:11-6.

11. Cao PP, Zhang YN, Liao B, Ma J, Wang BF, Wang H, et al. Increased local IgE production induced by common aeroallergens and phenotypic alteration of mast cells in Chinese eosinophilic, but not non-eosinophilic, chronic rhinosinusitis with nasal polyps. Clin Exp Allergy 2014; 44:690-700.

12. Gevaert P, Nouri-Aria KT, Wu H, Harper CE, Takhar P, Fear DJ, et al. Local receptor revision and class switching to IgE in chronic rhinosinusitis with nasal polyps. Allergy 2013; 68:55-63.

13. Mechtcheriakova D, Sobanov Y, Holtappels G, Bajna E, Svoboda M, Jaritz M, et al. Activation-induced cytidine deaminase (AID)-associated multigene signature to assess impact of AID in etiology of diseases with inflammatory component. PLoS One 2011; 6:e25611.

14. Gevaert P, Holtappels G, Johansson SG, Cuvelier C, Cauwenberge P, Bachert C. Organization of secondary lymphoid tissue and local IgE formation to

573 Staphylococcus aureus enterotoxins in nasal polyp tissue. Allergy 2005;
574 60:71-9.
575 15. Zhang YN, Song J, Wang H, Wang H, Zeng M, Zhai GT, et al. Nasal
576 IL-4(+)CXCR5(+)CD4(+) T follicular helper cell counts correlate with local
577 IgE production in eosinophilic nasal polyps. J Allergy Clin Immunol 2016;
578 137:462-73.
579 16. Lau A, Lester S, Moraitis S, Ou J, Psaltis AJ, McColl S, et al. Tertiary
580 lymphoid organs in recalcitrant chronic rhinosinusitis. J Allergy Clin Immunol
581 2017; 139:1371-3 e6.
582 17. Cao PP, Li HB, Wang BF, Wang SB, You XJ, Cui YH, et al. Distinct
583 immunopathologic characteristics of various types of chronic rhinosinusitis in
584 adult Chinese. J Allergy Clin Immunol 2009; 124:478-84, 84 e1-2.
585 18. Manzo A, Paoletti S, Carulli M, Blades MC, Barone F, Yanni G, et al.
586 Systematic microanatomical analysis of CXCL13 and CCL21 in situ
587 production and progressive lymphoid organization in rheumatoid synovitis.
588 Eur J Immunol 2005; 35:1347-59.
589 19. Canete JD, Santiago B, Cantaert T, Sanmarti R, Palacin A, Celis R, et al.
590 Ectopic lymphoid neogenesis in psoriatic arthritis. Ann Rheum Dis 2007;
591 66:720-6.
592 20. Ma J, Shi LL, Deng YK, Wang H, Cao PP, Long XB, et al. CD8(+) T cells
593 with distinct cytokine-producing features and low cytotoxic activity in
594 eosinophilic and non-eosinophilic chronic rhinosinusitis with nasal polyps.

595 Clin Exp Allergy 2016; 46:1162-75.

596 21. Nayar S, Campos J, Chung MM, Navarro-Nunez L, Chachlani M, Steinthal N,
597 et al. Bimodal expansion of the lymphatic vessels is regulated by the
598 sequential expression of IL-7 and lymphotoxin alpha1beta2 in newly formed
599 tertiary lymphoid structures. J Immunol 2016; 197:1957-67.

600 22. Rangel-Moreno J, Carragher DM, de la Luz Garcia-Hernandez M, Hwang JY,
601 Kusser K, Hartson L, et al. The development of inducible bronchus-associated
602 lymphoid tissue depends on IL-17. Nat Immunol 2011; 12:639-46.

603 23. Tan BK, Klingler AI, Poposki JA, Stevens WW, Peters AT, Suh LA, et al.
604 Heterogeneous inflammatory patterns in chronic rhinosinusitis without nasal
605 polyps in Chicago, Illinois. J Allergy Clin Immunol 2017; 139:699-703 e7.

606 24. Bachert C, Gevaert P, Holtappels G, Johansson SG, van Cauwenberge P. Total
607 and specific IgE in nasal polyps is related to local eosinophilic inflammation. J
608 Allergy Clin Immunol 2001; 107:607-14.

609 25. Takhar P, Smurthwaite L, Coker HA, Fear DJ, Banfield GK, Carr VA, et al.
610 Allergen drives class switching to IgE in the nasal mucosa in allergic rhinitis. J
611 Immunol 2005; 174:5024-32.

612 26. Cameron L, Gounni AS, Frenkiel S, Lavigne F, Vercelli D, Hamid Q. S epsilon
613 S mu and S epsilon S gamma switch circles in human nasal mucosa following
614 ex vivo allergen challenge: evidence for direct as well as sequential class
615 switch recombination. J Immunol 2003; 171:3816-22.

616 27. Cameron L, Hamid Q, Wright E, Nakamura Y, Christodoulopoulos P, Muro S,

et al. Local synthesis of epsilon germline gene transcripts, IL-4, and IL-13 in allergic nasal mucosa after ex vivo allergen exposure. J Allergy Clin Immunol 2000; 106:46-52.

28. Upadhyay V, Fu YX. Lymphotoxin signalling in immune homeostasis and the control of microorganisms. Nat Rev Immunol 2013; 13:270-9.

29. Pitzalis C, Jones GW, Bombardieri M, Jones SA. Ectopic lymphoid-like structures in infection, cancer and autoimmunity. Nat Rev Immunol 2014; 14:447-62.

30. Drayton DL, Liao S, Mounzer RH, Ruddle NH. Lymphoid organ development: from ontogeny to neogenesis. Nat Immunol 2006; 7:344-53.

31. Drayton DL, Bonizzi G, Ying X, Liao S, Karin M, Ruddle NH. I kappa B kinase complex alpha kinase activity controls chemokine and high endothelial venule gene expression in lymph nodes and nasal-associated lymphoid tissue. J Immunol 2004; 173:6161-8.

32. Peters A, Pitcher LA, Sullivan JM, Mitsdoerffer M, Acton SE, Franz B, et al. Th17 cells induce ectopic lymphoid follicles in central nervous system tissue inflammation. Immunity 2011; 35:986-96.

33. Fleige H, Ravens S, Moschovakis GL, Bolter J, Willenzon S, Sutter G, et al. IL-17-induced CXCL12 recruits B cells and induces follicle formation in BALT in the absence of differentiated FDCs. J Exp Med 2014; 211:643-51.

34. Shi LL, Song J, Xiong P, Cao PP, Liao B, Ma J, et al. Disease-specific T-helper cell polarizing function of lesional dendritic cells in different types of

chronic rhinosinusitis with nasal polyps. Am J Respir Crit Care Med 2014; 190:628-38.

35. Vinuesa CG, Linterman MA, Yu D, MacLennan IC. Follicular helper T cells. Annu Rev Immunol 2016; 34:335-68.

36. Shinoda K, Hirahara K, Iinuma T, Ichikawa T, Suzuki AS, Sugaya K, et al. Thy1+IL-7+ lymphatic endothelial cells in iBALT provide a survival niche for memory T-helper cells in allergic airway inflammation. Proc Natl Acad Sci U S A 2016; 113:E2842-51.

37. Feldman S, Kasjanski R, Poposki J, Hernandez D, Chen JN, Norton JE, et al. Chronic airway inflammation provides a unique environment for B cell activation and antibody production. Clin Exp Allergy 2017; 47:457-66.

38. Pikor NB, Astarita JL, Summers-Deluca L, Galicia G, Qu J, Ward LA, et al. Integration of Th17- and lymphotoxin-derived signals initiates meningeal-resident stromal cell remodeling to propagate neuroinflammation. Immunity 2015; 43:1160-73.

39. Litsiou E, Semitekolou M, Galani IE, Morianos I, Tsoutsa A, Kara P, et al. CXCL13 production in B cells via Toll-like receptor/lymphotoxin receptor signaling is involved in lymphoid neogenesis in chronic obstructive pulmonary disease. Am J Respir Crit Care Med 2013; 187:1194-202.

40. Frija-Masson J, Martin C, Regard L, Lothe MN, Touqui L, Durand A, et al. Bacteria-driven peribronchial lymphoid neogenesis in bronchiectasis and cystic fibrosis. Eur Respir J 2017; 49. pii: 1601873. doi:

10.1183/13993003.01873-2016.

41. GeurtsvanKessel CH, Willart MA, Bergen IM, van Rijt LS, Muskens F, Elewaut D, et al. Dendritic cells are crucial for maintenance of tertiary lymphoid structures in the lung of influenza virus-infected mice. J Exp Med 2009; 206:2339-49.

42. Wu X, Mimms R, Lima R, Peters-Hall J, Rose MC, Pena MT. Localization of inflammatory mediators in pediatric sinus mucosa. Arch Otolaryngol Head Neck Surg 2012; 138:389-97.

43. Schlosser RJ, Mulligan JK, Hyer JM, Karnezis TT, Gudis DA, Soler ZM. Mucous cytokine levels in chronic rhinosinusitis-associated olfactory loss. JAMA Otolaryngol Head Neck Surg 2016; 142:731-7.

44. Xin J, Sun H, Kong H, Li L, Zheng J, Yin C, et al. Intercellular adhesion molecule-1 expression in activated eosinophils is associated with mucosal remodeling in nasal polyps. Mol Med Rep 2015; 11:3391-7.

45. Eweiss A, Dogheim Y, Hassab M, Tayel H, Hammad Z. VCAM-1 and eosinophilia in diffuse sino-nasal polyps. Eur Arch Otorhinolaryngol 2009; 266:377-83.

46. Tomassen P, Vandeplas G, Van Zele T, Cardell LO, Arebro J, Olze H, et al. Inflammatory endotypes of chronic rhinosinusitis based on cluster analysis of biomarkers. J Allergy Clin Immunol 2016; 137:1449-56 e4.

47. Wang X, Zhang N, Bo M, Holtappels G, Zheng M, Lou H, et al. Diversity of TH cytokine profiles in patients with chronic rhinosinusitis: A multicenter

study in Europe, Asia, and Oceania. J Allergy Clin Immunol 2016; 138:1344-53.

Table 1. Structures of lymphoid aggregates in nasal polyps

		Number of samples analyzed	T/B segregation, n (%)	PNAd+ HEV, n (%)	CXCL13, n (%)	CCL21, n (%)	CD21, n (%)	Ki-67, n (%)
Grade 1	ENP	18	5 (27.77%)	3 (16.67%)	2 (11.11%)	2 (11.11%)	0 (0%)	0 (0%)
	NENP	14	3 (21.42%)	2 (14.29%)	1 (7.14%)	1 (7.14%)	0 (0%)	0 (0%)
Grade 2	ENP	6	4 (66.67%)	5 (83.33%)	6 (100%)	6 (100%)	3 (50%)	5 (83.33%)
	NENP	8	6 (75%)	6 (75%)	7 (87.5%)	7 (87.5%)	6 (75%)	6 (75%)
Grade 3	ENP	8	7 (87.5%)	8 (100%)	8 (100%)	8 (100%)	7 (87.5%)	8 (100%)
	NENP	5	5 (100%)	5 (100%)	5 (100%)	5 (100%)	5 (100%)	5 (100%)

Grade corresponds to the highest grade of lymphoid aggregation present in a nasal polyp sample.

FIGURE LEGENDS

720 **Figure 1**. Structures of eLTs in nasal polyps. **A, (**a) Representative photomicrographs
721 showing consecutive tissue sections stained for $CD3^+$ T cells, $CD20^+$ B cells, $CD21^+$
722 follicular DCs, and Ki-67^+ proliferating cells. Original magnification × 100; (b)
723 Higher magnification of the outlined area of (a). **B,** (a) Representative
724 photomicrographs showing $PNAd^+$ HEVs, D2-40^+ lymphatic vessels, $CD11c^+$
725 myeloid DCs (mDCs), $CD138^+$ plasma cells, $CD68^+$ macrophages, and $CD56^+$ nature
726 killer cells. Original magnification × 200; (b) Higher magnification of the outlined
727 area of (a). **C,** Representative photomicrographs showing Ki-67^+ B cells in polyp eLTs**.**
728 Original magnification × 200. Arrows denote Ki-67^+ B cells. **D,** Localization of
729 mDCs in eLTs. Representative photomicrographs showing consecutive tissue sections
730 stained for CD3 and CD11c, and CD3 and CD20. Original magnification × 200.
731 Arrow denotes close contact between T cells and mDCs. In (C) and (D), insets show a
732 higher magnification of the outlined area.

733

734 **Figure 2.** Increased formation of eLTs in NPs.

735

736 **Figure 3.** Increased expression of homeostatic chemokines and chemokine receptors
737 in NPs with eLTs. **A,** The mRNA levels of homeostatic chemokines and chemokine
738 receptors. eLTs-, without eLTs; eLTs+, with eLTs. *P < 0.05; **P < 0.01; ***P <
739 0.001. **B,** Representative photomicrographs showing staining for CXCL13 and CD21,
740 and CXCL13 and CD20 in polyp eLTs. Original magnification × 200. **C,** (a)
741 Representative photomicrographs showing staining for CCL21 in polyp eLTs.

Original magnification × 100; (b) Higher magnification of the outlined area of (a). **D,** Representative photomicrographs showing staining for CXCR5 and CD20, and CCR7 and CD3 in polyp eLTs. Original magnification × 200. In (B) and (D), insets show a higher magnification of the outlined area and arrows denote positive cells.

Figure 4. Increased expression of lymphorganogenic factors and adhesion molecules in NPs with eLTs. **A,** The mRNA levels of lymphorganogenic factors and adhesion molecules. eLTs-, without eLTs; eLTs+, with eLTs. $*P < 0.05$; $**P < 0.01$; $***P < 0.001$. **B,** (a) Representative photomicrographs showing polyp tissue sections stained for LTα, LTβ and LTβR. Original magnification × 100; (b) Higher magnification of the outlined area of (a). **C and D,** Representative photomicrographs showing staining for (C) LTβR and CD20, IL-17A, and IL-7, and (D) VCAM1 and ICAM1 in polyp eLTs. Original magnification × 200. Insets show a higher magnification of the outlined area. Arrows denote positive cells.

Figure 5. Presence of cellular and molecular components required for immunoglobulin production in eLTs in NPs. **A,** Identification of $CXCR5^+CD4^+$ TFH cells in B-cell follicles of polyp eLTs. Representative photomicrographs showing the staining of consecutive sections. Original magnification × 200. **B,** (a) Gating strategy and representative flow plots; (b) The frequencies of different types of cells in nasal mucosal mononuclear cells (NMCs) or in $CD4^+$ T cells; (c) The percentages of TFH cell subsets in NMCs. **C**, The mRNA expression levels of AID, CD21L, and BAFF.

764 eLTs-, without eLTs; eLTs+, with eLTs. *P < 0.05; **P < 0.01; ***P < 0.001. **D,** (a)
765 Representative photomicrographs showing the staining for AID, BAFF, and Bcl-2.
766 Original magnification × 200; (b) Higher magnification of the outline area of (a). **E,**
767 Representative photomicrographs showing staining for CD23 and CD20, and CD23
768 and CD21. Original magnification × 200. In (A) and (E), insets show a higher
769 magnification of the outlined area and arrows denote positive cells.
770
771 **Figure 6.** Increased local immunoglobulin production in NPs with eLTs. **A,** The local
772 protein levels of immunoglobulins. **B,** Representative photomicrographs showing
773 staining for immunoglobulins, CD20, and CD138. Original magnification × 200. **C,**
774 Representative photomicrographs showing staining for IgE, CD21, and tryptase.
775 Original magnification × 200. In (B) and (C), insets show a higher magnification of
776 the outlined area and arrows denote positive cells. **D,** Representative pictures of
777 electrophoresis results of semi-nested PCR assay of specific circle transcript of Iε-Cμ
778 (408 bp) in polyp tissues following *ex vivo* Der p1 challenge. Lanes M, +C, -C
779 correspond to marker, PCR positive control, and negative control. PCR amplification
780 of mRNA isolated from tonsil B cells stimulated with IL-4 and soluble CD40L was
781 used as positive control. A 'no template' sample was used as negative control. eLTs-,
782 without eLTs; eLTs+, with eLTs. *P < 0.05; **P < 0.01; ***P < 0.001.
783

784 **Figure 7**. Schematic overview of histological structure and immunoglobulin
785 production supporting function of eLT in NPs, and potential mechanisms underlying
786 lymphoid neogenesis in NPs.

787

788

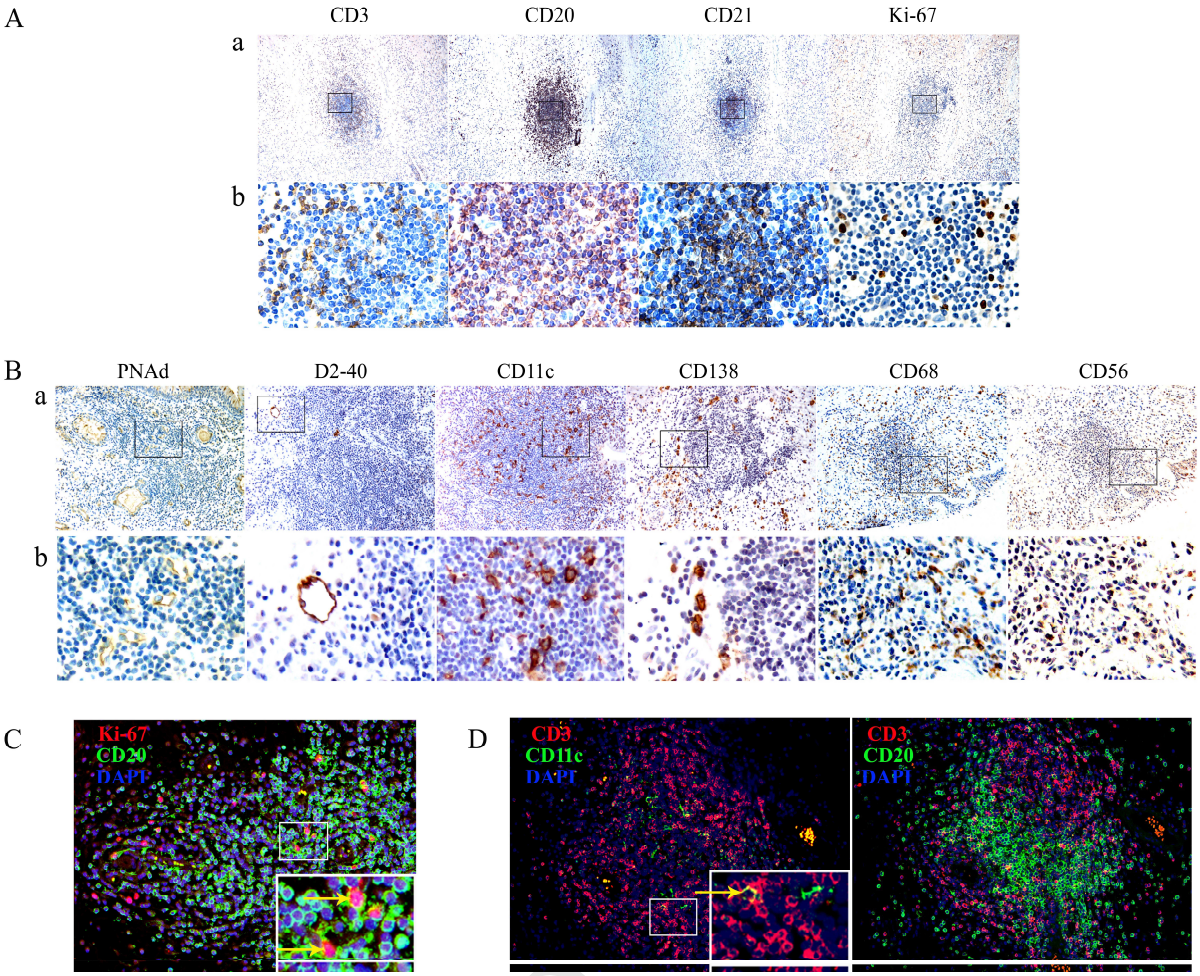

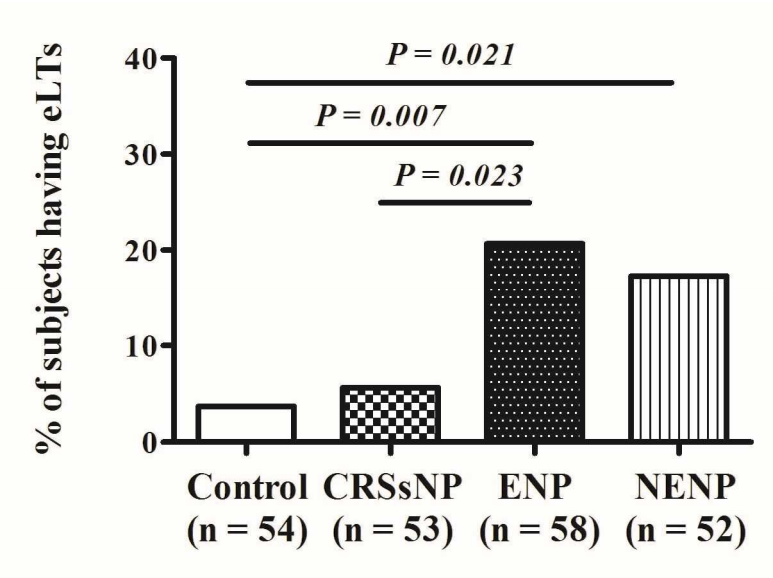

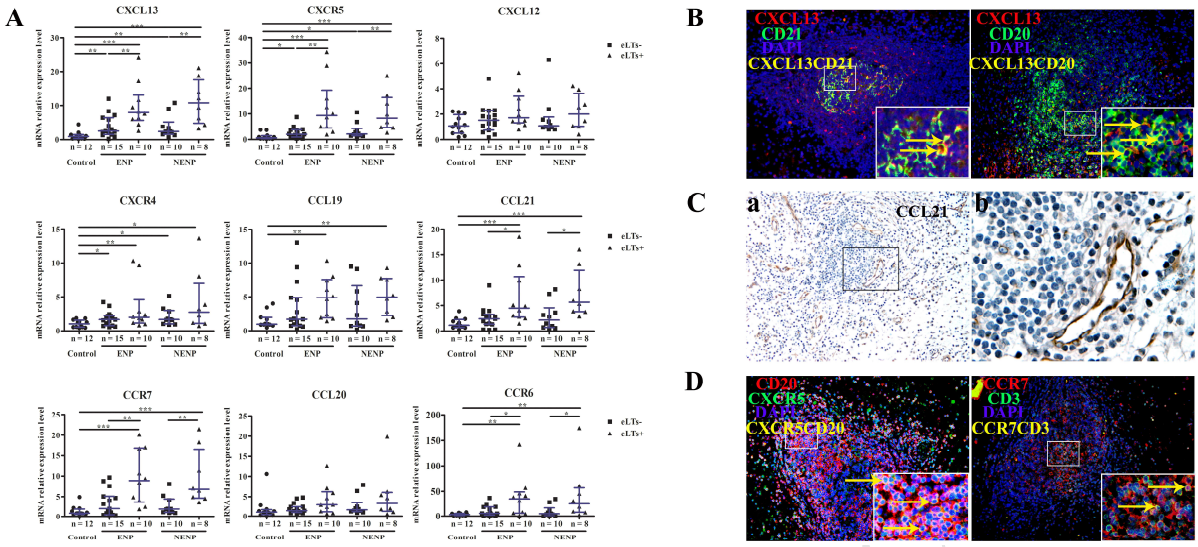

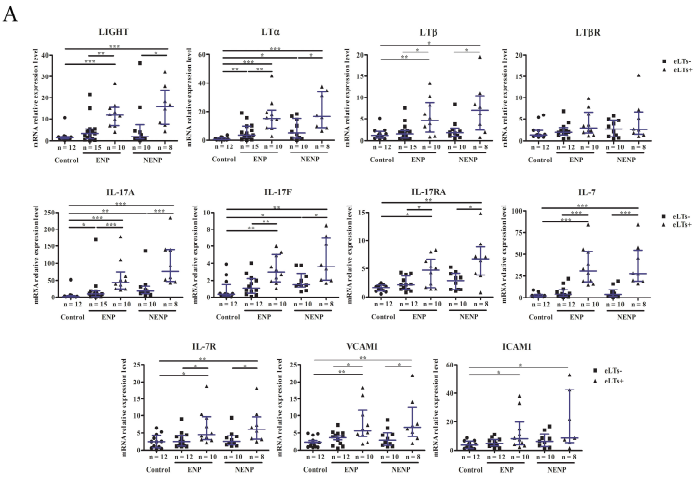

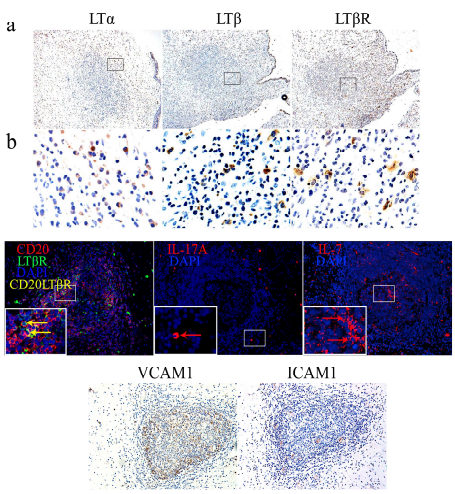

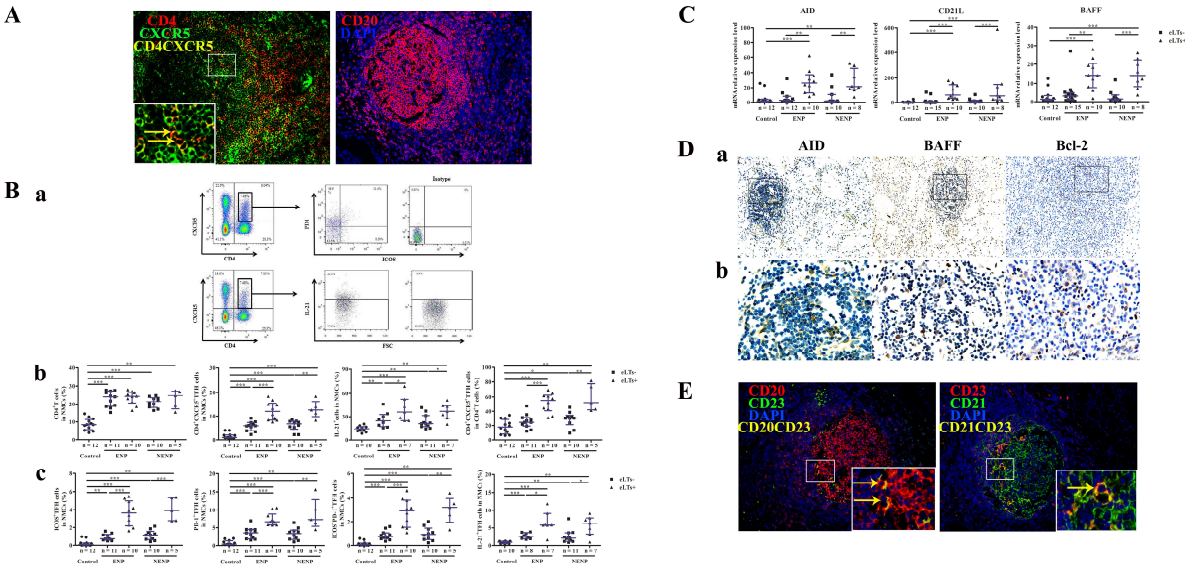

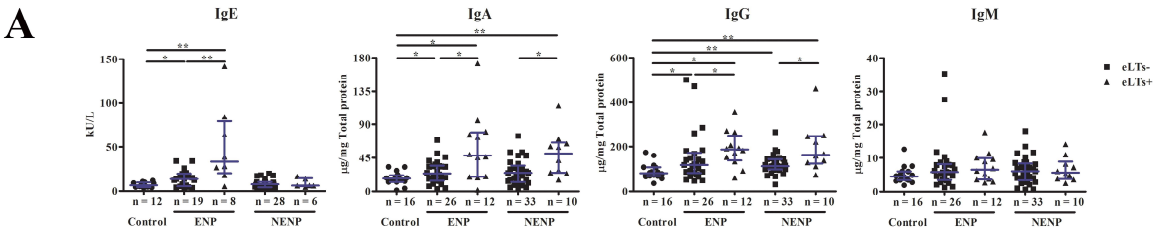
A
IgE
IgA
IgG
IgM
kU/L
μg/mg Total protein
eLTs-
eLTs+
n = 12
n = 19
n = 8
n = 28
n = 6
n = 16
n = 26
n = 12
n = 33
n = 10
Control
ENP
NENP

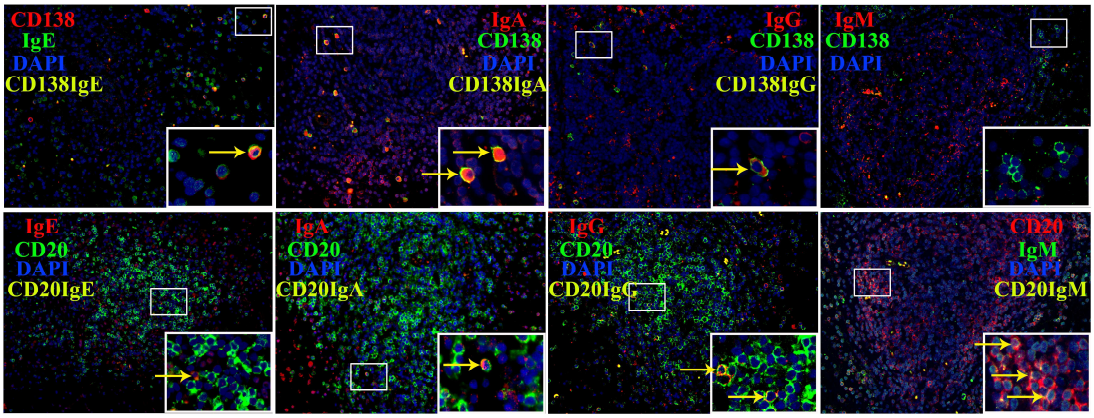
B
CD138
IgE
DAPI
CD138IgE
IgA
CD138
DAPI
CD138IgA
IgG
CD138
DAPI
CD138IgG
IgM
CD138
DAPI
IgE
CD20
DAPI
CD20IgE
IgA
CD20
DAPI
CD20IgA
IgG
CD20
DAPI
CD20IgG
CD20
IgM
DAPI
CD20IgM

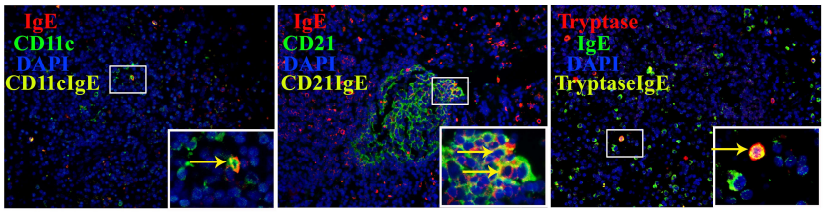
C
IgE
CD11c
DAPI
CD11cIgE
IgE
CD21
DAPI
CD21IgE
Tryptase
IgE
DAPI
TryptaseIgE

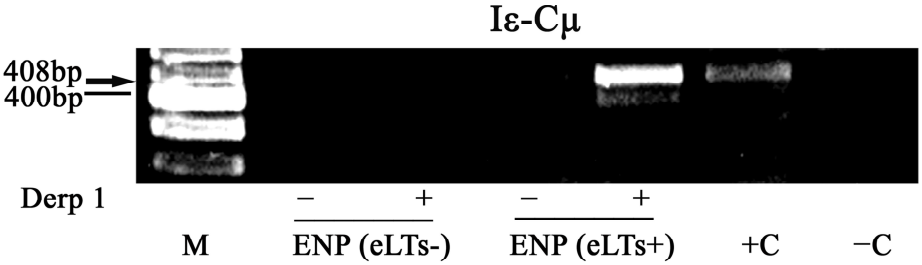
D
Iε-Cμ
408bp
400bp
Derp 1
−
+
−
+
M
ENP (eLTs-)
ENP (eLTs+)
+C
−C

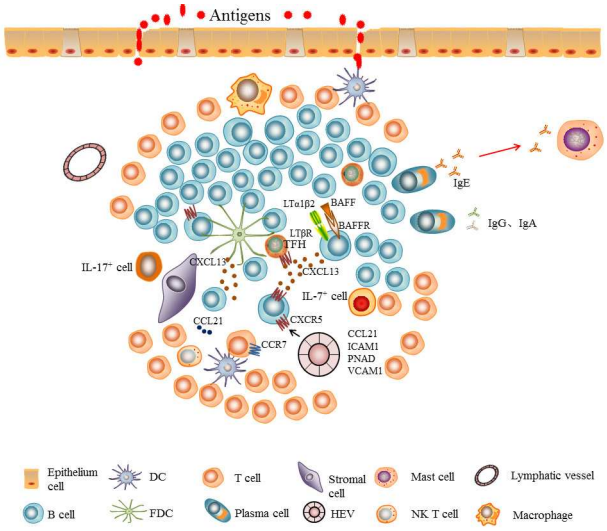

Online Repository

Ectopic Lymphoid Tissues Support Local Immunoglobulin Production in Chronic Rhinosinusitis with Nasal Polyps

Jia Song, M.D.[1*], Hai Wang, M.D.[1*], Ya-Na Zhang, M.D., Ph.D.[2], Ping-Ping Cao, M.D., Ph.D.[1], Bo Liao, M.D., Ph.D.[1], Zhe-Zheng Wang, M.D.[1], Li-Li Shi, M.D., Ph.D.[1], Yin Yao, M.D.[1], Guan-Ting Zhai, M.D.[1], Zhi-Chao Wang, M.D.[1], Li-Meng Liu[3], Ming Zeng, M.D., Ph.D.[1] , Xiang Lu, M.D., Ph.D.[1], Heng Wang, M.D., Ph.D.[1], Xiang-Ping Yang, Ph.D.[4], Di Yu, Ph.D.[5], Claus Bachert, M.D., Ph.D.[6], Zheng Liu, M.D., Ph.D.[1]

[1]Department of Otolaryngology-Head and Neck Surgery, Tongji Hospital, Tongji Medical College, Huazhong University of Science and Technology, Wuhan, P.R. China

[2]Department of Otolaryngology-Head and Neck Surgery, Guangzhou Women and Children's Medical Center, Guangzhou, P.R. China

[3]Li-Meng Liu is a summer student from No.1 Middle School affiliated to Central China Normal University, Wuhan, P.R.China

[4]Department of Immunology, School of Basic Medicine, Tongji Medical College, Huazhong University of Science and Technology, Wuhan, P.R. China

[5]Department of Immunology and Infectious Disease, John Curtin School of Medical Research, Australian National University, Canberra, Australia

[6]Upper Airways Research Laboratory, Ghent University, Ghent, Belgium

* These authors contributed equally to the completion of this article.

Running Head: eLTs in CRSwNP

For correspondence, please contact:

Zheng Liu, MD., Ph.D.

Department of Otolaryngology-Head and Neck Surgery

Tongji Hospital, Tongji Medical College

Huazhong University of Science and Technology

No. 1095 Jiefang Avenue

Wuhan 430030, P.R.China

E-mail: zhengliuent@hotmail.com

METHODS

Subjects and specimens

This study was approved by the Ethics Committee of Tongji Hospital of Huazhong University of Science and Technology and was conducted with written informed consent from each patient. A total of 103 patients with eosinophilic chronic rhinosinusitis with nasal polyps (CRSwNP), 171 patients with non-eosinophilic CRSwNP, 53 patients with chronic rhinosinusitis without nasal polyps (CRSsNP), and 135 subjects undergoing septoplasty without other sinonasal diseases were included in this study. Atopic status was evaluated by skin prick test to a standard panel of 16 aeroallergens in our region that was performed in accordance with WHO guideline.[E1, E2] Allergic rhinitis was diagnosed based on the concordance between a typical history of allergic symptoms and positive atopy test.[E3] The diagnosis of asthma was based on Global Initiative for Asthma guideline.[E4] Oral glucocorticoids and intranasal steroid sprays were discontinued at least 3 months and 1 month before surgery, respectively. None had received anti-leukotrienes or immunotherapy. Subjects who had an antrochoanal polyp, cystic fibrosis, fungal sinusitis, primary ciliary dyskinesia, vasculitis, or an acute upper respiratory tract infection within 1 month of entering the study were excluded from the study. Computed tomography (CT) scans in the axial and coronal plane were obtained preoperatively and evaluated by using the Lund-Mackay CT scoring system as previously described.[E5] Subjective symptoms focused on nasal obstruction, rhinorrhea, loss of sense of smell, facial pain, and headache were scored on a visual analogue scale (VAS) of 0 to 10 as previously

described.[E5] The total VAS symptom scores were calculated based on the sum of these five VAS symptom domains. The overall disease burden was also scored on a VAS by asking patients how troublesome their disease was in affecting their daily activity and sleep.[E5] Endoscopy physical findings were scored according to Lanza and Kennedy.[E5]

Polyp tissues from CRSwNP patients, diseased sinus mucosa from CRSsNP patients, and inferior turbinate mucosa from control subjects were collected during surgery. Given the limited amount of tissue samples, not all samples were included in every study protocol. The demographic characteristics of CRSwNP and control subjects are summarized in Table E1. For CRSsNP patients, age (years) median was 36 (interquartile ranges, 24-55) and 37 (70%) of them were male. There were 9 atopic patients (17%), 5 (9%) patients with asthma, and 6 (11%) patients with allergic rhinitis in CRSsNP patient group.

Histology study

For each subject, 2-5 paraffin blocks of a sinonasal mucosal sample were randomly chosen. At least three sections (4 μm) from the anterior, middle and posterior portion of paraffin blocks were obtained for histology study. Sections were stained with hematoxylin-eosin to screen the presence of lymphoid aggregates by two independent investigators. In the case of disagreement, a consensus was reached by reviewing the specimen at a multi-head microscope by these two investigators.[E6] Aggregates featuring a global count of less than 15 cells were not considered.[E7] Lymphocyte aggregation was graded according to a previously described method.[E7,

[E8] Each sample was graded according to the highest level of lymphoid aggregation present.[E7, E8] Cell aggregates with a radial cell count between 2 and 5 cells are classified as Grade 1.[E7, E8] Grade 2 aggregates have a radial cell count from 6 to 10 cells, while Grade 3 aggregates have more than 10 radial cells.[E7, E8] The radial cell count was estimated by counting the number of cells from the central point to the identifiable edge of each aggregate with the widest infiltration (Fig E1, A).[E7] The number of lymphoid aggregates was counted at a low power magnification (× 100), and 5 low power fields (LPFs) were randomly selected and analyzed.

Immunohistochemistry and immunofluorescence

After screening the presence of lymphoid aggregates in tissues by hematoxylin-eosin staining, additional adjacent tissue sections were prepared for immunohistochemical and immunofluorescence staining. Immunohistochemistry and immunofluorescence were performed as previously described.[E6, E9-11] After deparaffinization and rehydration, sections were subjected to heat-induced antigen retrieval using Target Retrieval Solution (Dako, Carpinteria, Calif, USA). The 5% bovine serum albumin was used to block nonspecific binding. Primary antibodies used are listed in Table E2. Fluorescence conjugated secondary antibodies used are listed in Table E3. For immunohistochemical staining, the streptavidin-biotin-peroxidase complex detecting method (Boster Biotechnology, Wuhan, China) was employed and color development was achieved with 3', 3'-diaminobenzidine.[E6, E9] Structures of lymphoid aggregates were evaluated by

staining sections for CD3, CD20, CD21, CD23, CD11c, CD138, CD68, CD56, Ki-67, B-cell lymphoma 2 (Bcl-2), activation-induced cytidine deaminase (AID), peripheral node addressin (PNAd), and D2-40. In addition, the expression of lymphorganogenic factors including chemokine (C-X-C motif) ligand 13 (CXCL13)/C-X-C chemokine receptor 5 (CXCR5), chemokine (C-C motif) ligand 21 (CCL21)/C-C chemokine receptor 7 (CCR7), lymphotoxin α (LTα), lymphotoxin β (LTβ), LTβ receptor (LTβR), B cell-activating factor of the tumor necrosis factor family (BAFF), IL-17A, IL-7, intercellular adhesion molecule 1 (ICAM1), and vascular cell adhesion molecule 1 (VCAM1) as well as the immunoglobulin (Ig) positive cells including IgE-, IgA-, IgG-, and IgM-expressing cells were assessed by immunohistochemistry and immunofluorescence. Germinal center (GC)-like structures were defined as T and B cell aggregates with Ki-67$^+$ proliferating B cells, a network of CD21$^+$ follicular dendritic cells (FDCs), and development of high endothelial venules (HEVs).[E12] Human tonsil tissues were used as positive controls for immunohistochemistry and immunofluorescence (Fig E2). Images were recorded with PS software (Photoshop, Adobe systems, San Jose, California, USA). Species and subtype-matched antibodies were used as negative controls.

Measurement of Igs and cytokines

Tissue samples were weighted and homogenized, and the supernatants were harvested.[E13] The protein levels of IgA, IgG, and IgM in tissue homogenates were detected by means of Bio-Plex suspension chip technology (BIO-RAD, Hercules, CA,

USA),[E13] and the lower detection limits are listed in Table E4. Tissue total IgE and specific IgE to *Dermatophagoides pteronyssinus* group 1 (Der p1) were detected by using ImmunoCAP system (Phadia, Uppsala, Sweden) as previously reported.[E14, E15] The lower detection limit for IgE was 0.35 kU/L. An ELISA-based chemiluminescent custom-made Q-Plex Custom array (Quansys Bioscience, West Logan, UT, USA) was used to detect the levels of various cytokines in supernatants of tissue explant culture,[E16] and the lower detection limits are listed in Table E5. Tissue CXCL13, CCL21, and lymphotoxin α (LTα) were detected by using ELISA (MultiSciences, Hanzhou, China) following the instructions of manufacturer,[E17] and the lower detection limits are listed in Table E6. The levels of IgA, IgG, IgM, CXCL13, CCL21, and LTα in tissues were normalized to total tissue protein levels quantified by using a BCA protein detection kit (Guge Biotechnology, Wuhan, China).[E13, E18]

Reverse transcription polymerase chain reaction

As mentioned elsewhere,[E6, E14] total RNA was extracted by using TRIzol (Invitrogen Life Technologies, Carlsbad, California, USA) and reverse-transcribed to cDNA by using a PrimeScript RT reagent kit (TaKaRa Biotechnology, Dalian, China). Real-time PCR was carried out using SYBR Premix Ex Taq kit (TaKaRa Biotechnology, Dalian, China) with appropriate primers (Table E7) on Light-Cycler system (Roche Diagnostics, Mannheim, Germany). Relative gene expression was calculated by using 2(-Delta Delta CT) method.[E6, E14] An inferior turbinate sample from a control subject was used as a calibrator. Glucuronidase-β (GUSB) or β-actin

was used as a housekeeping gene for normalization and a 'no template' sample was used as negative control. As previously described, the specific circle transcripts, Iε-Cμ (product resulting from class-switch recombination from IgM to IgE) and Iε-Cγ (product resulting from any IgG subclass to IgE) as well as Iε-Cγ1, Iε-Cγ3 and Iε-Cγ4 (products resulting from specific IgG subclass to IgE), were detected using semi-nested PCR amplification protocol with appropriate primers (Table E8).[E14] The first cycle was conducted at 94 ºC for 5 min, followed by 40 cycles of 94 ºC for 1 min, 66 ºC for 1 min, and 72 ºC for 1 min. The second round PCR was performed on a 5 μL aliquot of the first round PCR product with the same condition as mentioned above, except for the annealing temperature of 60 ºC. For each sample cDNA equivalent to 40 ng of total RNA was used. PCR amplification of mRNA isolated from tonsil B cells stimulated with IL-4 (200 U/mL, R&D systems, Minneapolis, Minn, USA) and soluble CD40L (0.1 μg/mL, R&D) for 5 days was used as positive control for circle transcript expression. A 'no template' sample was used as negative control. The semi-nested PCR products were subjected to agarose gel electrophoresis and visualized by ultraviolet transillumination.

Ex vivo allergen challenge

Sinonasal mucosal samples were used for *ex vivo* air-liquid interface culture as described previously.[E19] Sections of tissues of approximately 6 mm^3 were placed on 0.4-μm well inserts (Millipore Corp., Billerica, MA, USA) in 2 mL of Dulbecco's modified Eagle's medium/F-12 supplemented with 2 mM glutamine, 100 U/mL

177 penicillin, and 100 μg/mL streptomycin (Invitrogen, Carlsbad, CA, USA). The tissue
178 samples were oriented with the epithelium being exposed to the air, forming an
179 air-liquid interface to mimic the *in vivo* situation. Following the previously described
180 method,[E19, E20] the tissues were stimulated with recombinant Der p1 (20 μg/mL;
181 endotoxin ≤ 0.03 EU/μg; Indoor Biotechnologies, Charlottesville, VA, USA) and
182 cultured at 37 °C with 5% CO_2 in humidified air for 24 hours. After culture, tissues
183 and supernatants were harvested for semi-nested PCR and ELISA analysis,
184 respectively.
185
186 **Flow cytometry**
187 Sinonasal mucosal samples were dissociated mechanically with the
188 GentleMACS Dissociator (Miltenyi Biotec Technology & Trading (Shanghai) Co.
189 Shanghai, China).[E13] The resulting cell suspension was filtered through a mesh of 40
190 μm twice and then the nasal mucosal mononuclear cells (NMCs) were isolated by
191 density-gradient centrifugation on Lymphoprep (AXIS-SHIELD PoC AS, Oslo,
192 Norway) as previously described.[E9, E13] The viability of generated NMCs was greater
193 than 97% as detected by propidium iodide (MultiSciences Biotech, Hangzhou, China)
194 staining.[E13] Lymphocytes were defined, and debris, dead cells, and aggregates were
195 excluded, by forward angle and side scatter gating. Cells were surface stained for
196 CD4, inducible costimulator (ICOS), programmed cell death protein (PD1), and
197 CXCR5 with specific antibodies at 4°C for 30 minutes.[E13] For intracellular IL-21
198 staining, NMCs were cultured in the presence of Cell Stimulation Cocktail containing

protein transport inhibitors (eBioscience, San Diego, CA, USA) in RPMI 1640 medium (Invitrogen Life Technologies, Carlsbad, CA, USA) at 37°C for 12 hours and then fixed and permeabilized with Cytofix/Cytoperm Kit (Invitrogen Life Technologies). After that, cells were stained with mouse monoclonal antibodies against IL-21.[E13] Species and subtype-matched antibodies were used as controls. TFH cells were identified as $CXCR5^{+}CD4^{+}$ cells. In gated TFH cells, the expression of PD1, ICOS and IL-21 was analyzed. The primary antibodies used are listed in Table E9. The stained cells were analyzed on a FACS Calibur flow cytometer (Beckton Dickinson, San Jose, CA, USA) and data were analyzed using FlowJo software (TreeStar, Ashland, OR, USA).

REFERENCES

E1. Dong X, Huang N, Li W, Hu L, Wang X, Wang Y, et al. Systemic reactions to dust mite subcutaneous immunotherapy: A 3-year follow-up study. Allergy Asthma Immunol Res 2016; 8: 421-7.

E2. Bousquet J, Lockey R, Malling HJ. Allergen immunotherapy: therapeutic vaccines for allergic diseases. A WHO position paper. J Allergy Clin Immunol 1998; 102:558-62.

E3. Bousquet J, Khaltaev N, Cruz AA, Denburg J, Fokkens WJ, Togias A, et al. Allergic Rhinitis and its Impact on Asthma (ARIA) 2008 update (in collaboration with the World Health Organization, GA(2)LEN and AllerGen). Allergy 2008; 63 Suppl 86:8-160.

E4. Bateman ED, Hurd SS, Barnes PJ, Bousquet J, Drazen JM, FitzGerald M, et al. Global strategy for asthma management and prevention: GINA executive summary. Eur Respir J 2008; 31:143-78.

E5. Fokkens WJ, Lund VJ, Mullol J, Bachert C, Alobid I, Baroody F, et al. European Position Paper on Rhinosinusitis and Nasal Polyps 2012. Rhinol Suppl 2012:3 p preceding table of contents, 1-298.

E6. Cao PP, Li HB, Wang BF, Wang SB, You XJ, Cui YH, et al. Distinct immunopathologic characteristics of various types of chronic rhinosinusitis in adult Chinese. J Allergy Clin Immunol 2009; 124:478-84, 84 e1-2.

E7. Manzo A, Paoletti S, Carulli M, Blades MC, Barone F, Yanni G, et al. Systematic microanatomical analysis of CXCL13 and CCL21 in situ

production and progressive lymphoid organization in rheumatoid synovitis. Eur J Immunol 2005; 35:1347-59.

E8. Canete JD, Santiago B, Cantaert T, Sanmarti R, Palacin A, Celis R, et al. Ectopic lymphoid neogenesis in psoriatic arthritis. Ann Rheum Dis 2007; 66:720-6.

E9. Ma J, Shi LL, Deng YK, Wang H, Cao PP, Long XB, et al. CD8(+) T cells with distinct cytokine-producing features and low cytotoxic activity in eosinophilic and non-eosinophilic chronic rhinosinusitis with nasal polyps. Clin Exp Allergy 2016; 46:1162-75.

E10. Nayar S, Campos J, Chung MM, Navarro-Nunez L, Chachlani M, Steinthal N, et al. Bimodal expansion of the lymphatic vessels is regulated by the sequential expression of IL-7 and lymphotoxin alpha1beta2 in newly formed tertiary lymphoid structures. J Immunol 2016; 197:1957-67.

E11. Rangel-Moreno J, Carragher DM, de la Luz Garcia-Hernandez M, Hwang JY, Kusser K, Hartson L, et al. The development of inducible bronchus-associated lymphoid tissue depends on IL-17. Nat Immunol 2011; 12:639-46.

E12. Park CS, Choi YS. How do follicular dendritic cells interact intimately with B cells in the germinal centre? Immunology 2005; 114:2-10.

E13. Zhang YN, Song J, Wang H, Wang H, Zeng M, Zhai GT, et al. Nasal IL-4(+)CXCR5(+)CD4(+) T follicular helper cell counts correlate with local IgE production in eosinophilic nasal polyps. J Allergy Clin Immunol 2016; 137:462-73.

E14. Cao PP, Zhang YN, Liao B, Ma J, Wang BF, Wang H, et al. Increased local IgE production induced by common aeroallergens and phenotypic alteration of mast cells in Chinese eosinophilic, but not non-eosinophilic, chronic rhinosinusitis with nasal polyps. Clin Exp Allergy 2014; 44:690-700.

E15. Bachert C, Gevaert P, Holtappels G, Johansson SG, van Cauwenberge P. Total and specific IgE in nasal polyps is related to local eosinophilic inflammation. J Allergy Clin Immunol 2001; 107:607-14.

E16. Rosser CJ, Dai Y, Miyake M, Zhang G, Goodison S. Simultaneous multi-analyte urinary protein assay for bladder cancer detection. BMC Biotechnol 2014; 14:24.

E17. Tan BK, Klingler AI, Poposki JA, Stevens WW, Peters AT, Suh LA, et al. Heterogeneous inflammatory patterns in chronic rhinosinusitis without nasal polyps in Chicago, Illinois. J Allergy Clin Immunol 2017; 139:699-703 e7.

E18. Liao B, Cao PP, Zeng M, Zhen Z, Wang H, Zhang YN, et al. Interaction of thymic stromal lymphopoietin, IL-33, and their receptors in epithelial cells in eosinophilic chronic rhinosinusitis with nasal polyps. Allergy 2015; 70:1169-80.

E19. Cameron L, Gounni AS, Frenkiel S, Lavigne F, Vercelli D, Hamid Q. S epsilon S mu and S epsilon S gamma switch circles in human nasal mucosa following ex vivo allergen challenge: evidence for direct as well as sequential class switch recombination. J Immunol 2003; 171:3816-22.

E20. Takhar P, Smurthwaite L, Coker HA, Fear DJ, Banfield GK, Carr VA, et al.

Allergen drives class switching to IgE in the nasal mucosa in allergic rhinitis. J Immunol 2005; 174:5024-32.

328 **Table E1. Demographic characteristics of enrolled subjects**

	Control	ENP	NENP	Control *vs* ENP *P value*	Control *vs* NENP *P value*	ENP *vs* NENP *P value*
Total subjects enrolled	135	103	171			
Methodology used						
Histology study						
Subject number	135	96	168			
Gender, male	100 (74%)	70 (73%)	101 (60%)	*0.844*	***0.011***	***0.036***
Age (years)	32 (23, 49)	43 (30, 56)	37 (20, 50)	*0.058*	*0.715*	*0.122*
Patients with atopy	18 (13%)	27 (28%)	32 (19%)	***0.005***	*0.183*	*0.089*
Patients with AR	0 (0)	20 (21%)	29 (17%)	***< 0.001***	***< 0.001***	*0.473*
Patients with asthma	0 (0)	16 (17%)	7 (4%)	***< 0.001***	***0.018***	***0.001***
Immunohistochemistry and immunofluorescence						
Subject number	54	58	52			
Gender, male	41 (76%)	43 (74%)	37 (71%)	*0.827*	*0.578*	*0.726*
Age (years)	30 (21, 49)	38 (25, 51)	36 (20, 49)	*0.079*	*0.211*	*0.658*
Patients with atopy	10 (19%)	14 (24%)	9 (17%)	*0.468*	*0.871*	*0.379*
Patients with AR	0 (0)	8 (14%)	7 (13%)	***0.006***	***0.006***	*0.960*
Patients with asthma	0 (0)	6 (10%)	3 (6%)	***0.028***	*0.115*	*0.495*
RT-PCR						
Subject number	12	26	23			
Gender, male	8 (67%)	18 (69%)	18 (78%)	*1.000*	*0.686*	*0.475*
Age (years)	24 (19, 42)	37 (23, 54)	35 (20, 51)	*0.071*	*0.055*	*0.755*
Patients with atopy	1 (8%)	7 (27%)	4 (17%)	*0.393*	*0.640*	*0.425*
Patients with AR	0 (0)	3 (12%)	3 (13%)	*0.538*	*0.536*	*1.000*
Patients with asthma	0 (0)	3 (12%)	1 (4%)	*0.538*	*1.000*	*0.612*

Flow cytometry						
Subject number	22	28	24			
Gender, male	15 (68%)	22 (79%)	17 (71%)	*0.406*	*0.845*	*0.521*
Age (years)	29 (18, 49)	39 (19, 62)	37 (20, 61)	*0.092*	*0.098*	*0.993*
Patients with atopy	4 (18%)	7 (25%)	5 (21%)	*0.734*	*1.000*	*0.722*
Patients with AR	0 (0)	7 (25%)	3 (13%)	***0.014***	*0.235*	*0.254*
Patients with asthma	0 (0)	1 (4%)	0 (0%)	*1.000*	-	*1.000*
Immunoglobulin measurement						
Subject number	16	38	43			
Gender, male	12 (75%)	29 (76%)	25 (58%)	*1.000*	*0.234*	*0.083*
Age (years)	31 (22, 56)	43 (27, 59)	41 (22, 62)	*0.125*	*0.122*	*0.508*
Patients with atopy	2 (13%)	12 (32%)	9 (21%)	*0.187*	*0.710*	*0.275*
Patients with AR	0 (0)	6 (16%)	6 (14%)	*0.163*	*0.176*	*0.816*
Patients with asthma	0 (0)	4 (11%)	3 (7%)	*0.306*	*0.556*	*0.701*
Ex vivo study						
Subject number	5	9	8			
Gender, male	3 (60%)	6 (67%)	5 (63%)	*1.000*	*1.000*	*1.000*
Age (years)	43 (29, 51)	44 (32, 48)	45.5 (37, 51)	*0.894*	*0.608*	*0.562*
Patients with atopy	0 (0)	1 (11%)	0 (0)	*1.000*	-	*1.000*
Patients with AR	0 (0)	1 (11%)	0 (0)	*1.000*	-	*1.000*
Patients with asthma	0 (0)	0 (0)	0 (0)	-	-	-

For continuous variables, results are expressed as medians and interquartile ranges. Categorical variables are summarized using percentage.

ENP, eosinophilic nasal polyp; NENP, non-eosinophilic nasal polyp; AR, allergic rhinitis

335 **Table E2. Primary antibodies used in immunohistochemistry and**

336 **immunofluorescence**

Antibody	Application	Species	Concentration	Clone ID	Reference	Source
CD11c	IHC, IF	Rabbit	1:100	EP1347Y	Ab52632	Abcam (Cambridge, MA,UK)
CD138	IHC, IF	Rabbit	Undiluted	EP201	ZA-0584	Zhongshan Golden Bridge Biotechnology (Beijing, China)
CD138	IF	Mouse	1:100	B-A38	Ab34164	Abcam
CD3	IHC, IF	Mouse	1:100	LN10	ZM-0417	Zhongshan Golden Bridge Biotechnology
CD4	IF	Goat	1:100	polyclonal	AF-379	R&D systems (Minneapolis, USA)
CD21	IHC, IF	Rabbit	Undiluted	EP64	ZA-0525	Zhongshan Golden Bridge Biotechnology
CD68	IHC	Mouse	Undiluted	KP1	ZM-0060	Zhongshan Golden Bridge Biotechnology
CD56	IHC	Rabbit	1:400	polyclonal	bs-0736R	Biosynthesis Biotechnology (Beijing, China)
CD20	IHC, IF	Rabbit	1:100	EP7	ZA-0549	Zhongshan Golden Bridge Biotechnology
CD20	IF	Mouse	1:100	L26	ZM-0039	Zhongshan Golden Bridge Biotechnology
D2-40	IHC	Mouse	Undiluted	D2-40	ZM-0465	Zhongshan Golden Bridge Biotechnology
CXCL13	IF	Goat	Undiluted	polyclonal	ZG-0601	Zhongshan Golden Bridge Biotechnology
Ki-67	IHC, IF	Rabbit	1:100	EP5	ZA-0502	Zhongshan Golden Bridge Biotechnology
AID	IHC	Rabbit	1:100	polyclonal	Ab59361	Abcam
LTα	IHC	Rabbit	1:100	polyclonal	HPA007729	Sigama-Aldrich (St. Louis, MO, USA)
LTβ	IHC	Rabbit	1:400	polyclonal	HPA048884	Sigama-Aldrich
LTβR	IHC, IF	Rabbit	1:600	polyclonal	GTX12264	GeneTex (Irvine, Southern California, USA)
CXCR5	IF	Mouse	1:100	51505	MAB190	R&D systems

CCR7	IF	Rabbit	1:200	polyclonal	C3241	Abcam
IL-7	IF	Rabbit	1:100	polyclonal	bs-1811R	Biosynthesis Biotechnology
CCL21	IHC	Rabbit	1:200	polyclonal	bs-1666R	Biosynthesis Biotechnology
CD23	IF	Mouse	1:100	UMAB101	ZM-0273	Zhongshan Golden Bridge Biotechnology
PNAd	IHC	Rat	1:25	MECA-79	120802	eBioscience (San Diego, Calif, USA)
Tryptase	IF	Mouse	1:100	AA1	Ab2378	Abcam
Bcl-2	IHC	Rabbit	1:200	E17	Ab32124	Abcam
BAFF	IHC	Rat	1:100	Buffy 2	Ab16081	Abcam
IL-17A	IHC, IF	Rabbit	1:100	polyclonal	bs-2140R	Biosynthesis Biotechnology
ICAM1	IHC	Rabbit	1:200	EP1442Y	Ab53013	Abcam
VCAM1	IHC	Rabbit	1:500	EPR5047	Ab134047	Abcam
IgA	IF	Rabbit	1:200	EPR5367-76	Ab124716	Abcam
IgM	IF	Rabbit	1:100	EPR5539-65-4	Ab134159	Abcam
IgG	IF	Rabbit	1:500	RIGG-69	Ab133470	Abcam
IgE	IF	Mouse	1:100	B3102E8	9160	SouthernBiotech (Birmingham, USA)
IgE	IF	Rabbit	Undiluted	polyclonal	Ab75673	Abcam

CXCL13, chemokine (C-X-C motif) ligand 13; AID，activation-induced cytidine deaminase; LT, lymphotoxin; LTβR, lymphotoxin beta receptor; CCL21, chemokine (C-C motif) ligand 21; PNAd, peripheral node addressin; Bcl-2, B cell lymphoma 2; Ig, immunoglobulin; CXCR5, C-X-C chemokine receptor 5; CCR7, C-C chemokine receptor 7; IL, interleukin; VCAM1, vascular cell adhesion molecule 1; ICAM1, intercellular adhesion molecule 1; BAFF, B cell-activating factor of the tumor

344 necrosis factor family; Ig, immunoglobulin; IHC, immunohistochemistry; IF,
345 immunofluorescence.
346
347
348
349
350
351
352
353
354
355
356
357
358
359
360
361
362
363
364
365

366 **Table E3. Secondary antibodies used in immunofluorescence**

Antibody	Concentration	Clone ID	Reference	Source
IFKine™ Green donkey anti-mouse IgG	1:100	polyclonal	A24211	Abbkine Scientific Company (Wuhan, China)
IFKine™ Red donkey anti-mouse IgG	1:100	polyclonal	A24411	Abbkine
IFKine™ Green donkey anti-rabbit IgG	1:100	polyclonal	A24221	Abbkine
IFKine™ Red donkey anti-rabbit IgG	1:100	polyclonal	A24421	Abbkine
IFKine™ Red donkey anti-goat IgG	1:100	polyclonal	A24431	Abbkine

367

368

369

370

371

372

373

374

375

376

377

378

379

380

381

Table E4. Detection limits for Bio-Plex assay.

Target	Detection limit
IgA	103.4 pg/mL
IgG	941.0 pg/mL
IgM	9.0 pg/mL

Ig, immunoglobulin.

Table E5. Detection limits for Q-Plex Custom array

Target	Detection limit
IL-4	2.68 pg/mL
IL-5	1.90 pg/mL
IL-7	1.35 pg/mL
IL-13	3.00 pg/mL
IL-17A	4.00 pg/mL
IL-21	1.50 pg/mL
LTα	0.60 pg/mL

IL, interleukin; LTα, lymphotoxin α.

Table E6. Detection limits for ELISA

Target	Detection limit
CXCL13	4.86 pg/mL
CCL21	2.60 pg/mL
LTα	2.02 pg/mL

CXCL13, chemokine (C-X-C motif) ligand 13; CCL21, chemokine (C-C motif) ligand 21; LTα, lymphotoxin α.

452 **Table E7. Primers used for quantitative RT-PCR analysis**

Primer	Sequence	Expected product size (bp)	Annealing temperature (°C)
CXCL12	(F) 5'-ATTCTCAACACTCCAAACTGTGC-3' (R) 5'-CTTCAGCCGGGCTACAATCTG-3'	48	60
CXCL13	(F) 5'-GGACTCAGAGCTCAAGTCTGAACTC-3' (R) 5'-CAGCAGCATGAGAAGCAGAGA-3'	78	60
CXCR4	(F) 5'-ACGCCACCAACAGTCAGAG-3' (R) 5'-AGTCGGGAATAGTCAGCAGGA-3'	96	60
CXCR5	(F) 5'-AACGTCCTGGTGCTGGTGA-3' (R) 5'-CACGGCAAAGGGCAAGA-3'	139	60
CCL19	(F) 5'-TGTCTGTGACCCAGAAACCCA-3' (R) 5'-TGAACACTACAGCAGGCACCC-3'	96	60
CCL20	(F) 5'-CTGTACCAAGAGTTTGCTCC-3' (R) 5'-GCACAATATATTTCACCCAAG-3'	251	62
CCL21	(F) 5'-GCCACACTCTTTCTCCTGCTTT-3' (R) 5'-ACTCTCCCTCCTCGGTCTCTCT-3'	109	65
CCR6	(F) 5'-TTCAGCGATGTTTTCGACTCC-3' (R) 5'-GCAATCGGTACAAATAGCCTGG-3'	134	62
CCR7	(F) 5'-TGAGGTCACGGACGATTACAT-3' (R) 5'-GTAGGCCCACGAAACAAATGAT-3'	143	60
IL-7	(F) 5'-TTGGACTTCCTCCCCTGATCC-3' (R) 5'-TCGATGCTGACCATTAGAACAC-3'	109	60
IL-7R	(F) 5'-CCCTCGTGGAGGTAAAGTGC-3' (R) 5'-CCTTCCCGATAGACGACACTC-3'	199	60
IL-17A	(F) 5'-TCCCACGAAATCCAGGATGC-3' (R) 5'-GGATGTTCAGGTTGACCATCAC-3'	75	60
IL-17F	(F) 5'-GCTGTCGATATTGGGGCTTG-3' (R) 5'-GGAAACGCGCTGGTTTTCAT-3'	160	60
IL-17RA	(F) 5'-GCTTCACCCTGTGGAACGAAT-3' (R) 5'-TATGTGGTGCATGTGCTCAAA-3'	98	60
VCAM1	(F) 5'-GGGAAGATGGTCGTGATCCTT-3' (R) 5'-TCTGGGGTGGTCTCGATTTTA-3'	89	60
ICAM1	(F) 5'-ATGCCCAGACATCTGTGTCC-3' (R) 5'-GGGGTCTCTATGCCCAACAA-3'	112	60
CD21L	(F) 5'-TGGAACCTGGGATAAACCTGC-3' (R) 5'-GACTTGTTTCCGTTCATGGAGA-3'	171	60
AID	(F) 5'-GAGGCGTGACAGTGCTACATC-3' (R) 5'-CAGGGTCTAGGTCCCAGTCC-3'	116	62
BAFF	(F) 5'-GGGAGCAGTCACGCCTTAC-3' (R) 5'-GATCGGACAGAGGGGCTTT-3'	103	60
LTα	(F) 5'-ATGACACCACCTGAACGTCTC-3'	241	60

LTβ	(R) 5'-CTCTCCAGAGCAGTGAGTTCT-3' (F) 5'-AGGGTGTACGTCAACATCAGTCA-3' (R) 5'-TATTCACGCACTCGCACCA-3'	118	60
LTβR	(F) 5'-AGACCTGCAGGGACCAGGAA-3' (R) 5'-ACAGCTGGCAGATGGTCAGGTA-3'	180	60
LIGHT	(F) 5'-ACTCTACAGTCACACCTATGGCATC -3' (R) 5'-AATCTGGCACTTCGCGTGTA-3'	104	60
GUSB	(F) 5'-GACACGCTAGAGCATGAGGG-3' (R) 5'-GGGTGAGTGTGTTGTTGATGG-3'	123	60
ACTB	(F) 5'-CTGGAACGGTGAAGGTGACA-3' (R) 5'-AAGGGACTTCCTGTAACAATGCA-3'	145	60

CXCL, chemokine (C-X-C motif) ligand; CXCR, C-X-C chemokine receptor; CCL, chemokine (C-C motif) ligand; CCR, C-C chemokine receptor; IL, interleukin; IL-7R, interleukin 7 receptor; IL-17RA, interleukin 17 receptor A; VCAM1, vascular cell adhesion molecule 1; ICAM1, intercellular adhesion molecule 1; LT, lymphotoxin; LTβR, lymphotoxin β receptor; BAFF, B cell-activating factor of tumor necrosis factor family; AID, activation-induced cytidine deaminase; CD21L, the long complement receptor type 2 isoform; LIGHT, tumor necrosis factor superfamily member 14; GUSB, beta-glucuronidase; ACTB, beta-actin.

Table E8 Primers used for semi-nested PCR analysis

Primer	Sequence	GenBank Accession No.
IεF1	5'-GGGAGCTGTCCAGGAACCCGACAGAGC-3'	X56797
IεF2	5'-GGCCACACATCCACAGGC-3'	X56797
CμR	5'-GTTGCCGTTGGGGTGCTGG-3'	X17115
CγR	5'-CCAACTCTCTTGTCCACCTTGG-3'	X04046
Cγ1R	5'-GGCATGTGTGAGTTTTGTCACAA-3'	J00228
Cγ3R	5'-GGCACGGGGGAGG-3'	X99549
Cγ4R	5'-GGGCATGGGGGACCATA-3'	KO1316

Iε-Cμ transcript was amplified by primer sets IεF1/CμR and IεF2/CμR. Iε-Cγ transcript was amplified by primer sets IεF1/CγR and IεF2/CγR. Iε-Cγ1, Iε-Cγ3, and Iε-Cγ4 transcript were amplified by primer sets IεF1/Cγ1R and IεF2/Cγ1R, IεF1/Cγ3R and IεF2/Cγ3R, and IεF1/Cγ4R and IεF2/Cγ4R, respectively.

Table E9. Primary antibodies used in flow cytometry

Antigen-Fluorophore	Manufacturer	Clone ID	Source	Isotype	Dilution
CD4-PE	eBioscience, San Diego, CA, USA	RPA-T4	mouse	IgG1, κ	1:20
CXCR5-Alexa Fluor 488	BD PharMingen, San Jose, CA, USA	RF8B2	rat	IgG2b, κ	1:20
ICOS-APC	eBioscience	ISA-3	mouse	IgG1, κ	1:20
PD1-PerCP/Cy5.5	eBioscience	J105	mouse	IgG1, κ	1:20
IL-21-APC	Biolegend, San Diego, CA, USA	3A3-N2	mouse	IgG1, κ	1:20

PE, phycoerythrin; APC, allophycocyanin; PerCP, peridinin chlorophyll protein complex; CXCR5, CXCR, C-X-C chemokine receptor 5; ICOS, inducible costimulator; PD1, programmed cell death protein.

Table E10. The frequencies of lymphoid aggregates in different study groups

	Overall lymphoid aggregates, n (%)	Grade 1, n (%)	Grade 2, n (%)	Grade 3, n (%)
Control (n = 135)	26 (19.26%)	18 (13.33%)	5 (3.70%)	3 (2.22%)
ENP (n = 96)	52 (54.17%)	32 (33.33%)	10 (10.42%)	10 (10.42%)
NENP (n = 168)	81 (48.21%)	42 (25.00%)	22 (13.10%)	17 (10.12%)

ENP, eosinophilic nasal polyps; NENP, non-eosinophilic nasal polyps.

Table E11. Detection of circle transcripts in different types of sinonasal tissues after *ex vivo* stimulation with Der p1

	Control	**ENP**		**NENP**	
	local sIgE- eLTs- n = 5	local sIgE+ eLTs+ n = 5	local sIgE+ eLTs- n = 4	local sIgE- eLTs+ n = 4	local sIgE- eLTs- n = 4
Iε-Cμ CT	0/5	4/5	0/4	0/4	0/4
Iε-Cγ, Iε-Cγ1, Iε-Cγ3, or Iε-Cγ4 CT	0/5	0/5	0/5	0/5	0/5

ENP, eosinophilic nasal polyps; NENP, non-eosinophilic nasal polyps; CT, circle transcript; sIgE, specific immunoglobulin E against Der p1; eLTs, ectopic lymphoid tissues.

Table E12. The association between ectopic lymphoid tissue formation and clinical characteristics in patients with nasal polyps

	NP eLTs- (n = 133)	**NP eLTs+ (n = 41)**	***P value***
Duration of the disease (years)	2 (0.5, 5)	5 (3, 10)	< ***0.001***
Nasal obstruction VAS scores	6 (4, 8)	8 (6, 9)	< ***0.001***
Rhinorrhea VAS scores	6 (3, 8)	5 (3, 5.5)	*0.690*
Headache VAS scores	2 (0, 4.75)	2 (0, 4)	*0.466*
Facial pain VAS scores	0 (0, 2)	0 (0, 2)	*0.681*
Loss of smell VAS scores	3 (0, 8)	5 (1.75, 8)	*0.411*
Total VAS scores	17 (12, 26.5)	19 (15, 24.25)	*0.434*
Overall burden VAS scores	6 (5, 8)	7 (5, 8)	*0.069*
Total endoscopic scores	8 (6, 10)	8 (6, 9)	*0.833*
Total CT scores	14 (8.5, 20)	13 (8, 22)	*0.845*
Patients with AR	25 (19%)	7 (17%)	*0.803*
Patients with asthma	14 (11%)	3 (7%)	*0.765*
Prior surgery	38 (29%)	20 (49%)	***0.023***

For continuous variables, results are expressed as medians and interquartile ranges.

Categorical variables are summarized using percentage.

NP, nasal polyp; eLTs, ectopic lymphoid tissues; eLTs-, without eLTs; eLTs+, with eLTs; VAS, visual analogue scale; CT, computed tomography; AR, allergic rhinitis.

Given to the limited amount of tissue samples, in this study, eLTs were defined as grade 2 and grade 3 lymphoid aggregates evaluated by hematoxylin and eosin staining. The rationality is based on our finding that the majority (over 78%) of grade 2 and grade 3 lymphoid aggregates could be defined as eLTs by immunohistochemistry (see table 1).

Figure Legends

Figure E1. Increased formation of lymphoid aggregates in various grades in nasal polyps (NPs). **A,** A schematic figure showing the radial cell counting. **B,** Representative photomicrographs showing lymphoid aggregates in different grades in NPs (original magnification × 200) and lymphoid follicle in tonsils (original magnification × 100) detected by hematoxylin-eosin staining. **C,** The percentages of subjects having lymphoid aggregates in different grades. Grade corresponds to the highest grade of lymphoid aggregations present in a sinonasal mucosal sample. *P < 0.05, compared with controls with aggregate in the same grade. **D,** The total numbers of lymphoid aggregates and the number of lymphoid aggregates in different grades per low power field (LPF) in different study groups. **E,** Representative photomicrograph showing lymphoid aggregates in different grades in one polyp sample (original magnification × 100). ENP, eosinophilic NPs; NENP, non-eosinophilic NPs.

Figure E2. Photomicrographs showing tonsil tissue sections stained for CD3, CD20, CD21, Ki-67, CCL21, CD138, IgE, IgM, IgG, IgA, Ki-67 and CD20, CD4 and CXCR5, CD20 and CD23, and CD21 and CD23 by immunohistochemistry or immunofluorescence. Tonsil tissue was employed as positive control for immunohistochemical and immunofluorescence staining. Original magnification × 200.

Figure E3. The protein levels of CXCL13, CCL21, and LTα in tissue homogenates detected by using ELISA. eLTs-, without ectopic lymphoid tissues; eLTs+, with ectopic lymphoid tissues; ENP, eosinophilic nasal polyps; NENP, non-eosinophilic nasal polyps. *$P < 0.05$; **$P < 0.01$; ***$P < 0.001$.

Figure E4. Representative photomicrographs showing scattered $CXCL13^+$ mononuclear cells and $CCL21^+$ stromal cells (original magnification × 400), and $CXCR5^+$ cells, $CCR7^+$ cells, and $LT\beta R^+$ cells (original magnification × 200) in other areas in addition to ectopic lymphoid tissues in nasal polyps detected by immunohistochemistry or immunofluorescence. Insets show a higher magnification of the outlined area. Arrows denote positive cells.

Figure E5. A, Increased number of $IL\text{-}17A^+$ cells in nasal polyps (NPs). **B,** Infiltration of $IL\text{-}17A^+$ cells in sinonasal mucosa. Representative photomicrographs are shown. Original magnification × 400. eLTs-, without ectopic lymphoid tissues; eLTs+, with ectopic lymphoid tissues; ENP, eosinophilic NPs; NENP, non-eosinophilic NPs. **$P < 0.01$; ***$P < 0.001$.

Figure E6. Immunofluorescence demonstrated $IL\text{-}7^+$ cells in other locations besides ectopic lymphoid tissues in polyps. Representative photomicrograph is shown. Original magnification × 200. Inset shows a higher magnification of the outlined area. Arrow denotes positive cells.

Figure E7. Distribution of ICAM1 and VCAM1 positive vessels in other areas in addition to ectopic lymphoid tissues in nasal polyps. Representative photomicrographs are shown. Original magnification × 400.

Figure E8. The frequencies of $ICOS^+$, $PD1^+$, $ICOS^+PD1^+$, and $IL\text{-}21^+$ T follicular helper (TFH) cells in total TFH cells in control tissues, and nasal polyps (NPs) with and without ectopic lymphoid tissues (eLTs) analyzed by flow cytometry. ENP, eosinophilic NPs; NENP, non-eosinophilic NPs; eLTs-, without eLTs; eLTs+, with eLTs . *$P < 0.05$; **$P < 0.01$; ***$P < 0.001$.

Figure E9. Significant positive correlations between the mRNA expression of CD21L and AID, BAFF and AID, and BAFF and CD21L in polyps with ectopic lymphoid tissues.

Figure E10. The levels of immunoglobulins (Igs) in control tissues, eosinophilic nasal polyps (ENP), and non-eosinophilic nasal polyps (NENP). *$P < 0.05$; **$P < 0.01$.

Figure E11. The fold changes of protein levels of IL-4, IL-5, IL-7, IL-13, IL-17A, IL-21, and LTα in supernatants of control tissue and eosinophilic polyp tissue explants stimulated with Der p 1 over those in supernatants of tissue explants from the same

patient without stimulation. ENP, eosinophilic nasal polyps; eLTs, ectopic lymphoid tissues; eLTs-, without eLTs; eLTs+, with eLTs.

Figure E12. The fold changes of protein levels of IL-4, IL-5, IL-7, IL-13, IL-17A, IL-21, and LTα in supernatants of control tissue and non-eosinophilic polyp tissue explants stimulated with Der p 1 over those in supernatants of tissue explants from the same patient without stimulation. NENP, non-eosinophilic nasal polyps; eLTs, ectopic lymphoid tissues; eLTs-, without eLTs; eLTs+, with eLTs.

Figure E13. No difference in the frequency of ectopic lymphoid tissue formation in normal inferior turbinate tissues and normal ethmoid tissues. Normal ethmoid tissues were collected from 23 patients (age, years, 29 (18, 47); 15 (65%) male) suffering from nasal trauma, mucocele of frontal or sphenoid sinus, or nasal tumors, and without ethmoid sinus inflammation on coronal computed tomography scanning and endoscopy. eLTs, ectopic lymphoid tissues.

A

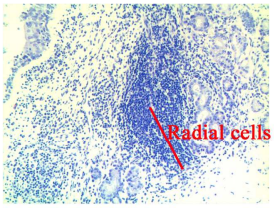

B

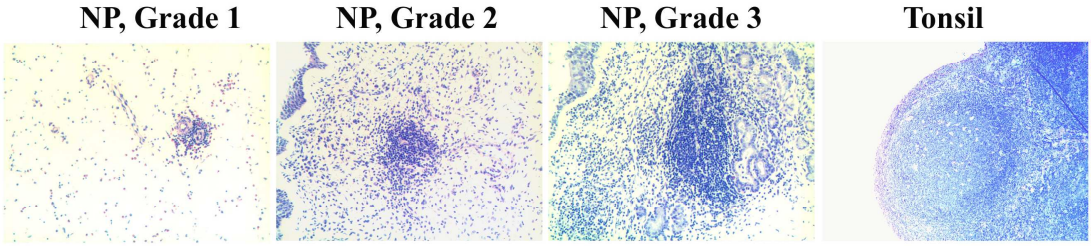

C

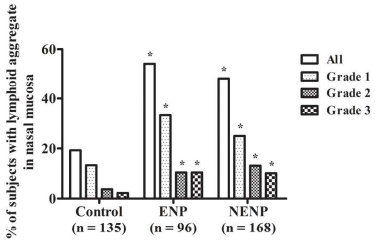

D

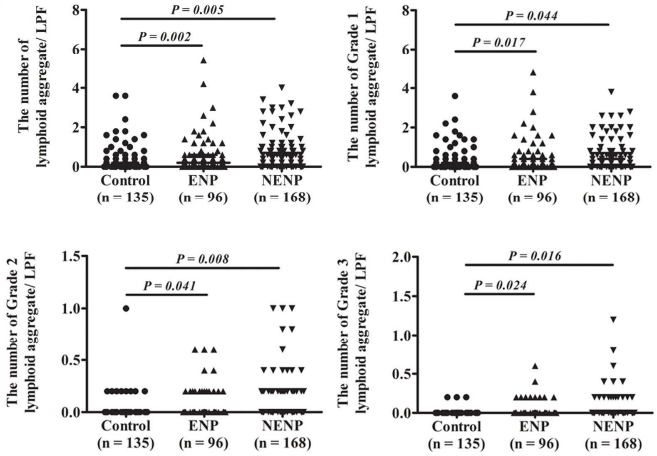

E

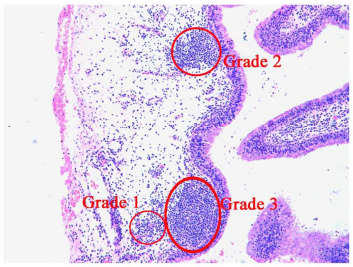

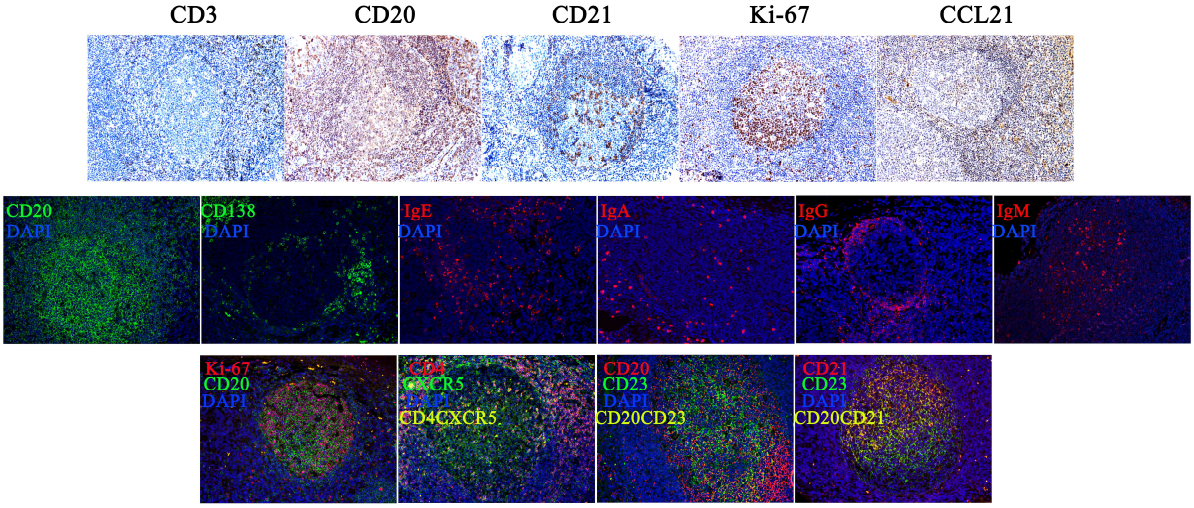

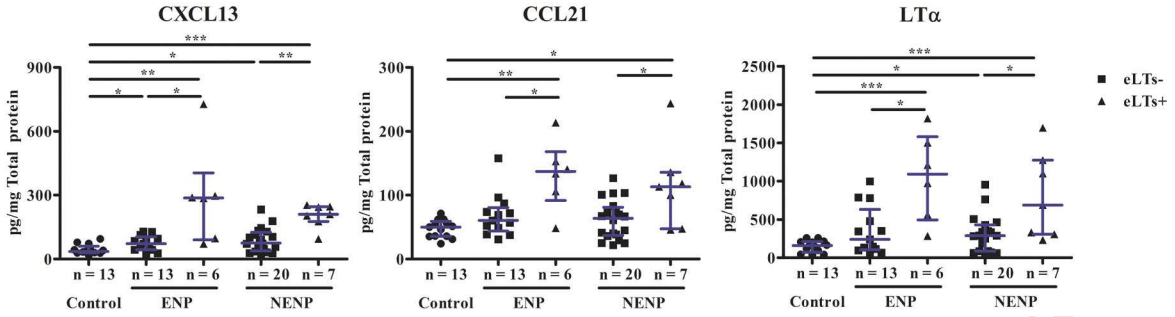

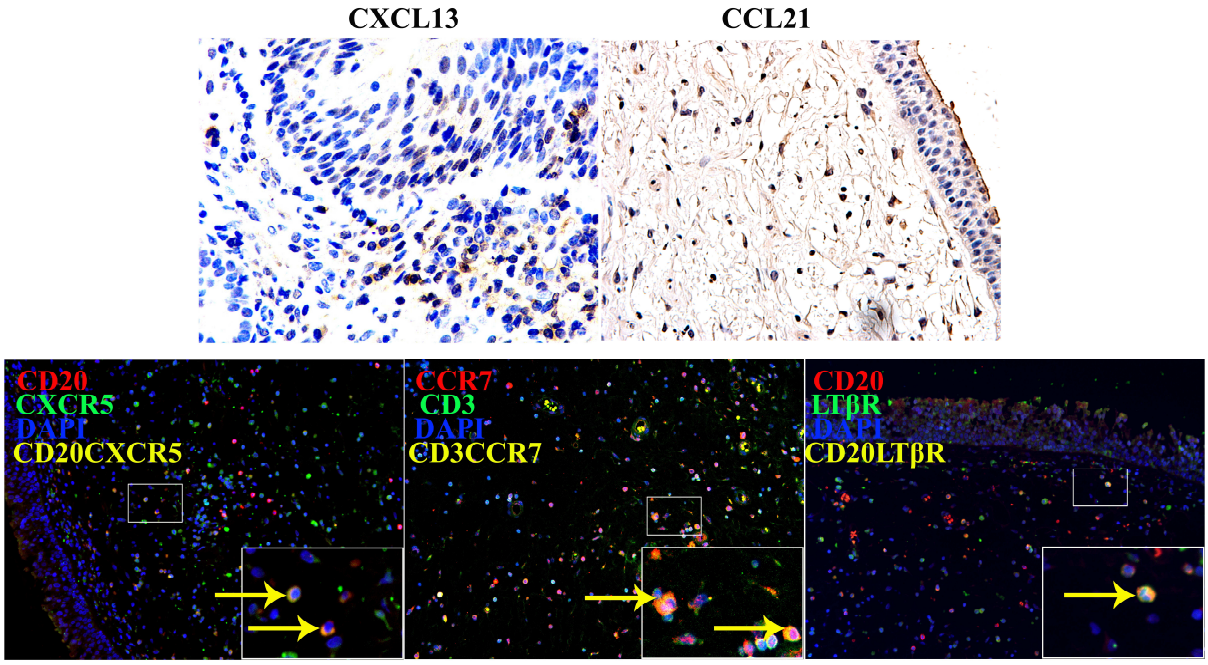

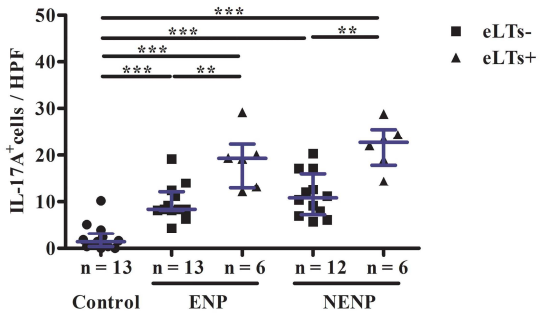

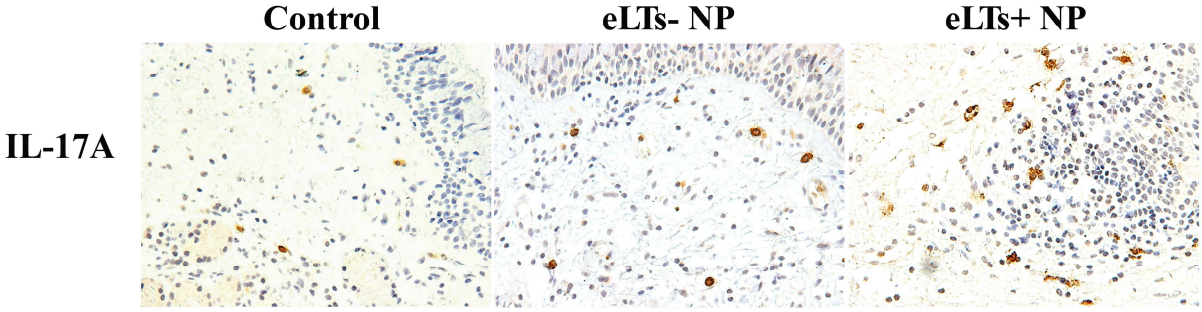

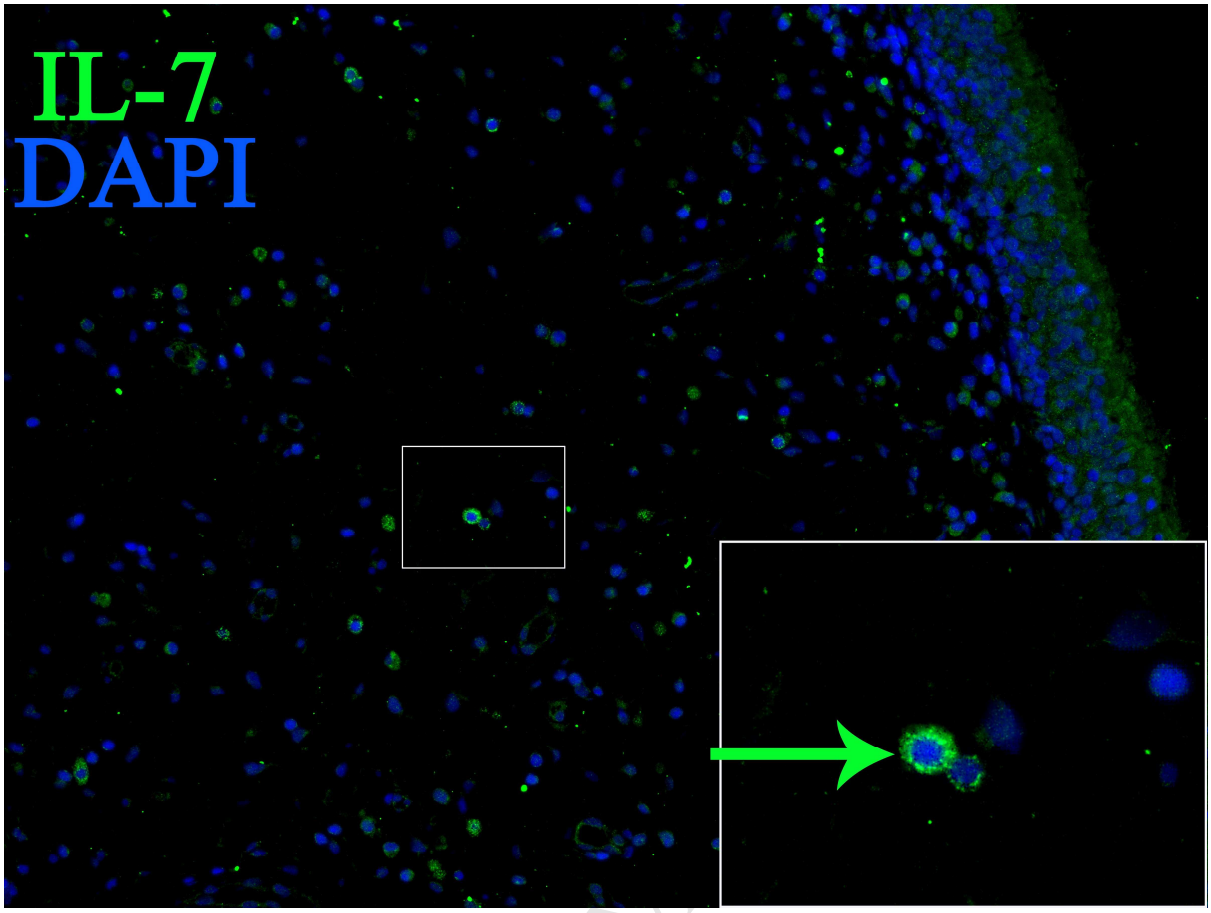

ICAM1

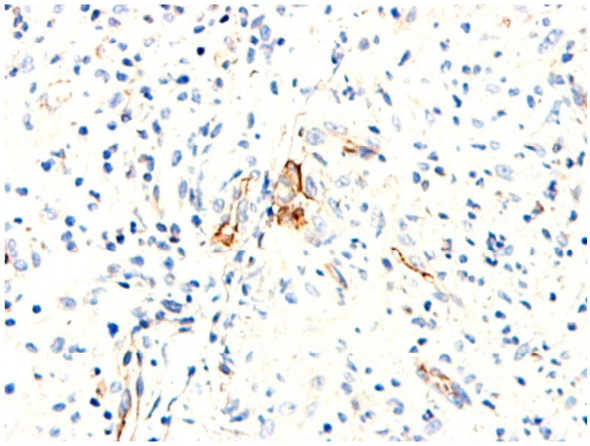

VCAM1